Detectors II: Tracking

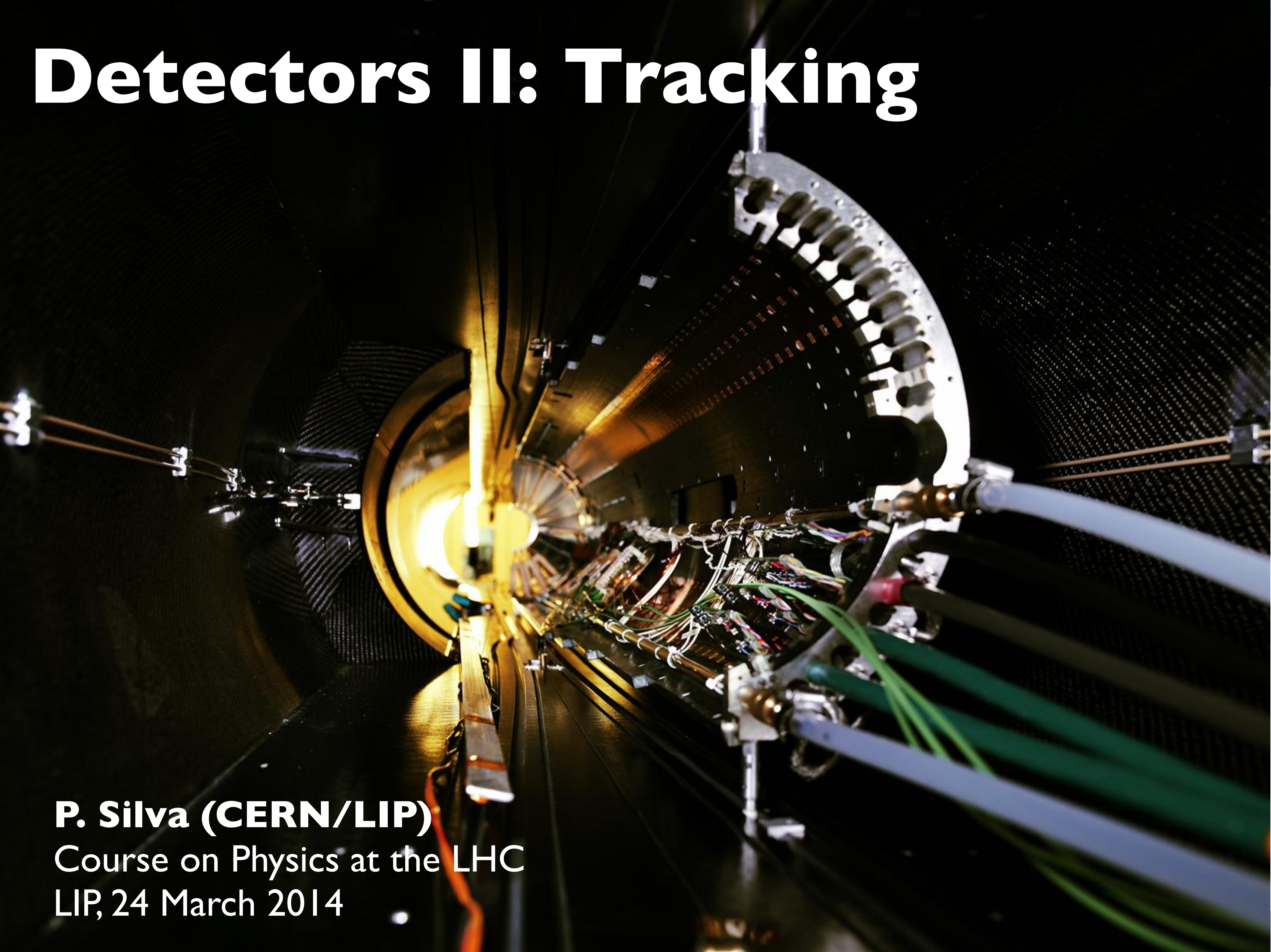

P. Silva (CERN/LIP)

Course on Physics at the LHC

LIP, 24 March 2014

Simplified overview of the LHC detectors concept

- **Inner tracking**
  - minimal interference with the event
  - identify and measure charged particles
- **Calorimetry**
  - absorb electromagnetic and hadronic E
  - avoid leakages → hermetic
- **Outer tracking**
  - Weakly interacting charged particles: muons
- **Magnetic field**
  - Field integral: B.r
  - Crucial for particle separation and p measurement

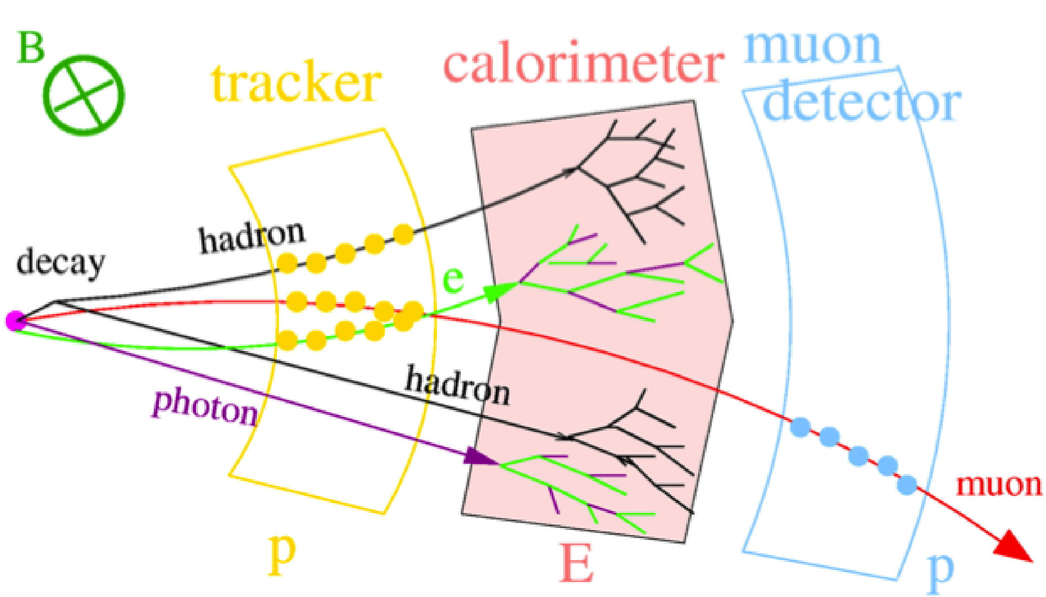

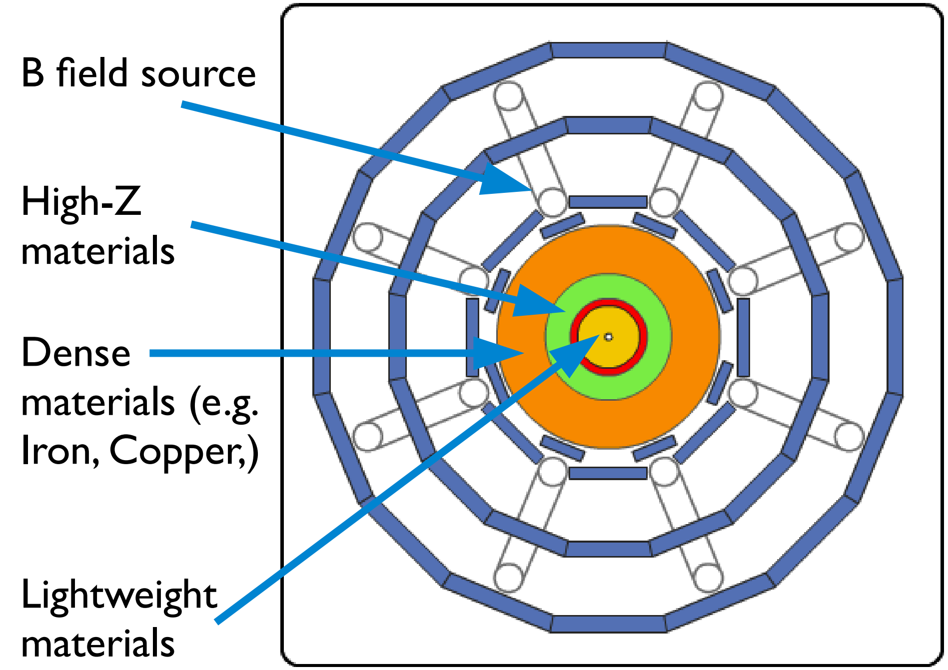

Particles and their decays

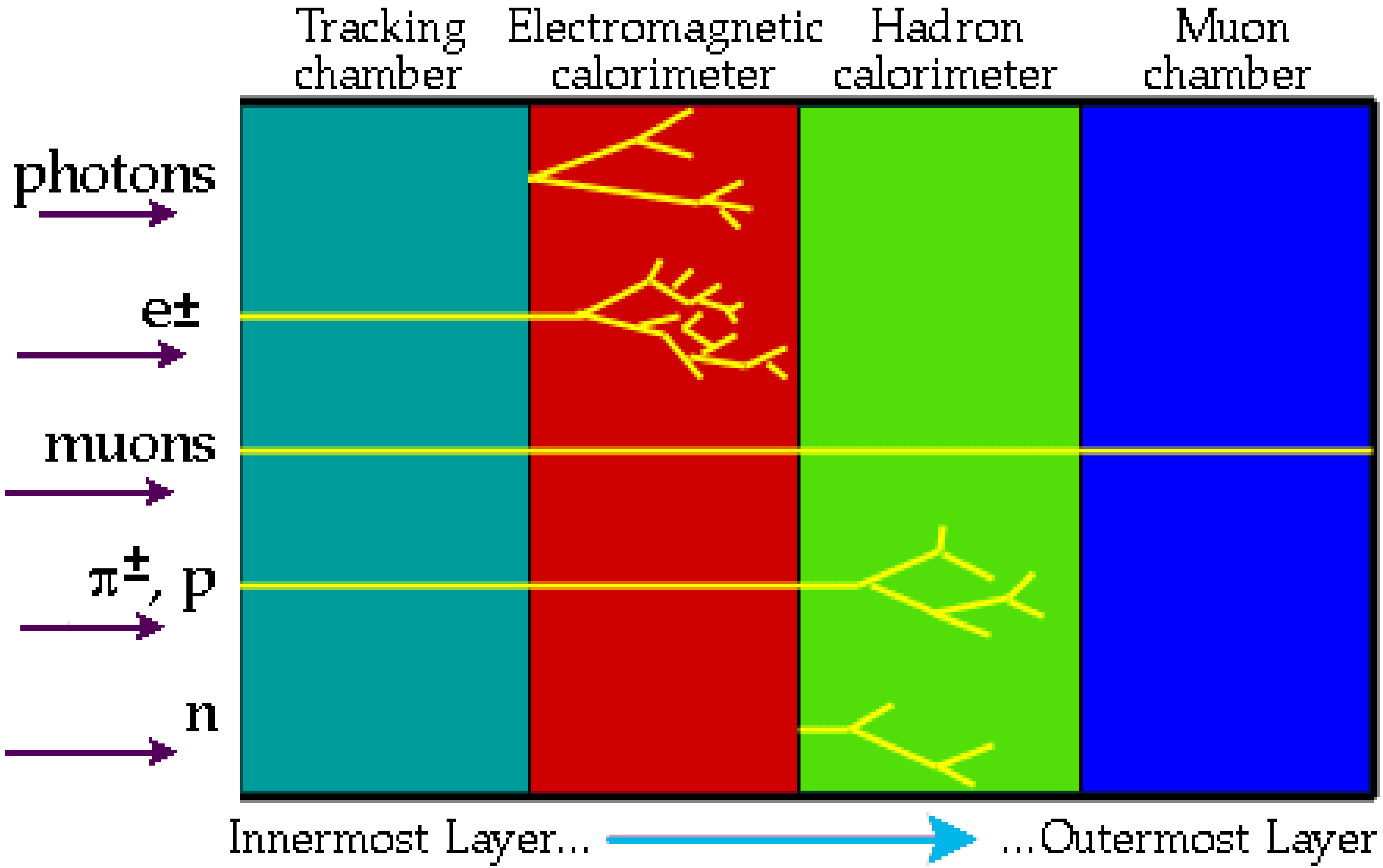

Particles and their decays

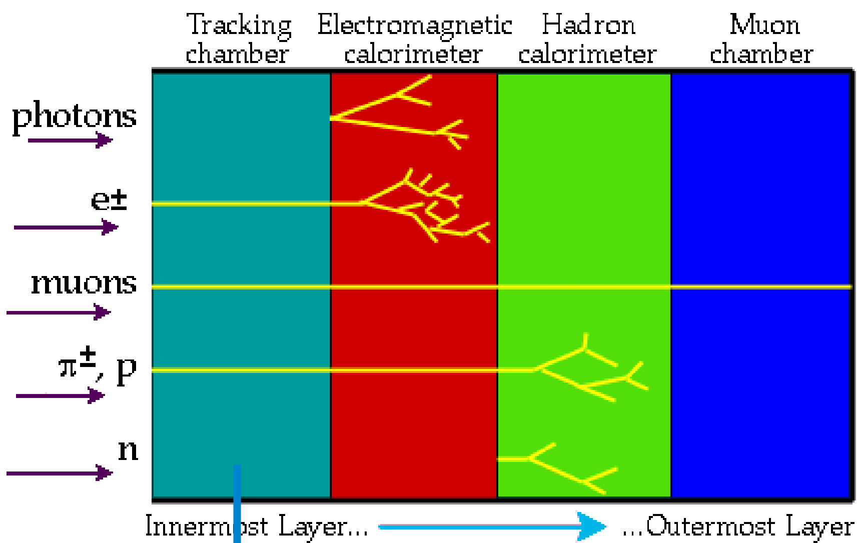

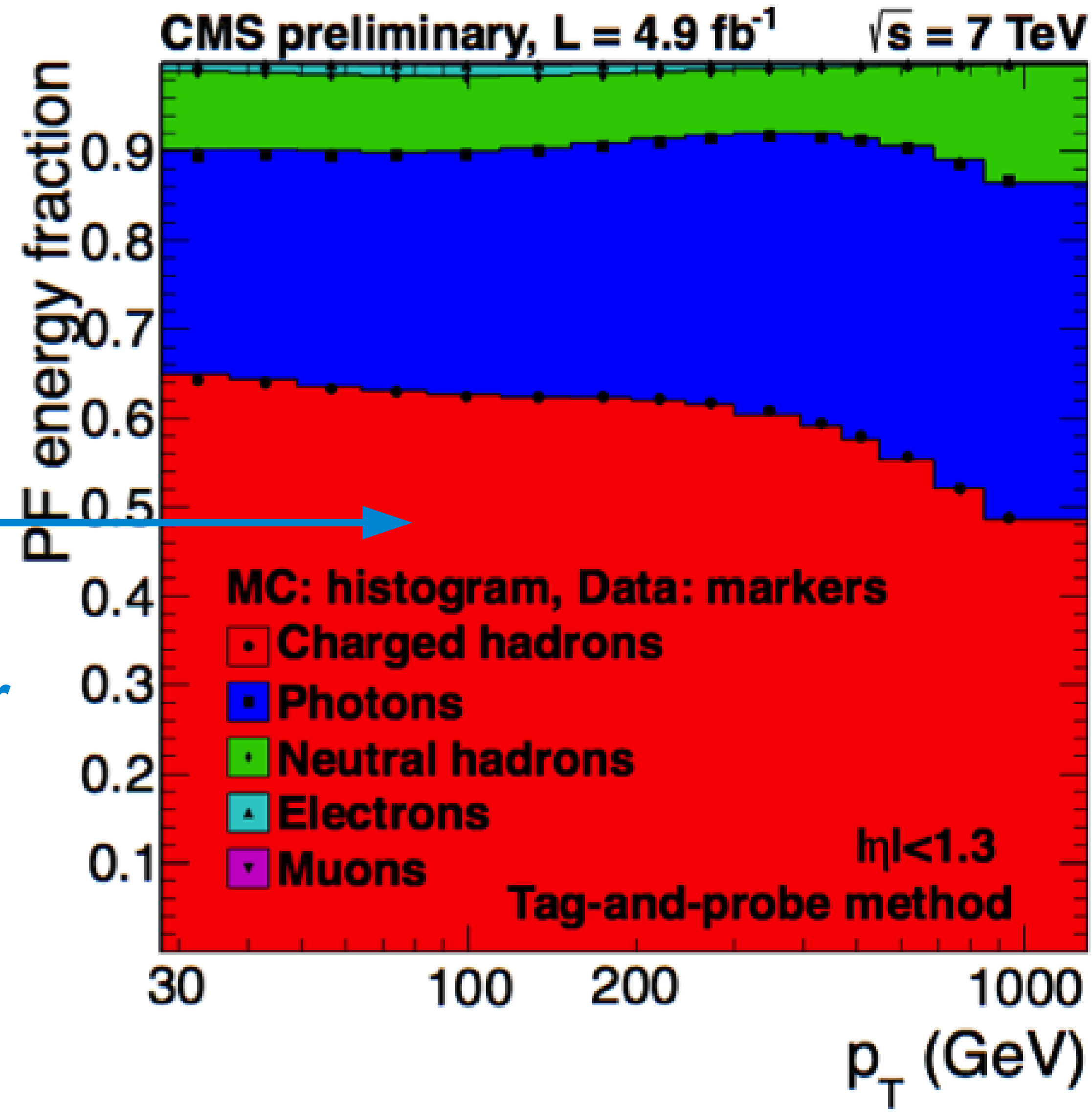

>60% of the energy of a jet may be reconstructed at the level of the tracker

Tracking: why?

- Identify the **hard interaction vertex**
- Reconstruct **secondary vertices** from long lived particles
- Measure **particle trajectories**
  - Momentum (p)
  - Energy loss (dE/dx)
  - Link to calorimeters (identify electrons, conversions)
  - Link to muon chambers : inner leg for muon reconstruction

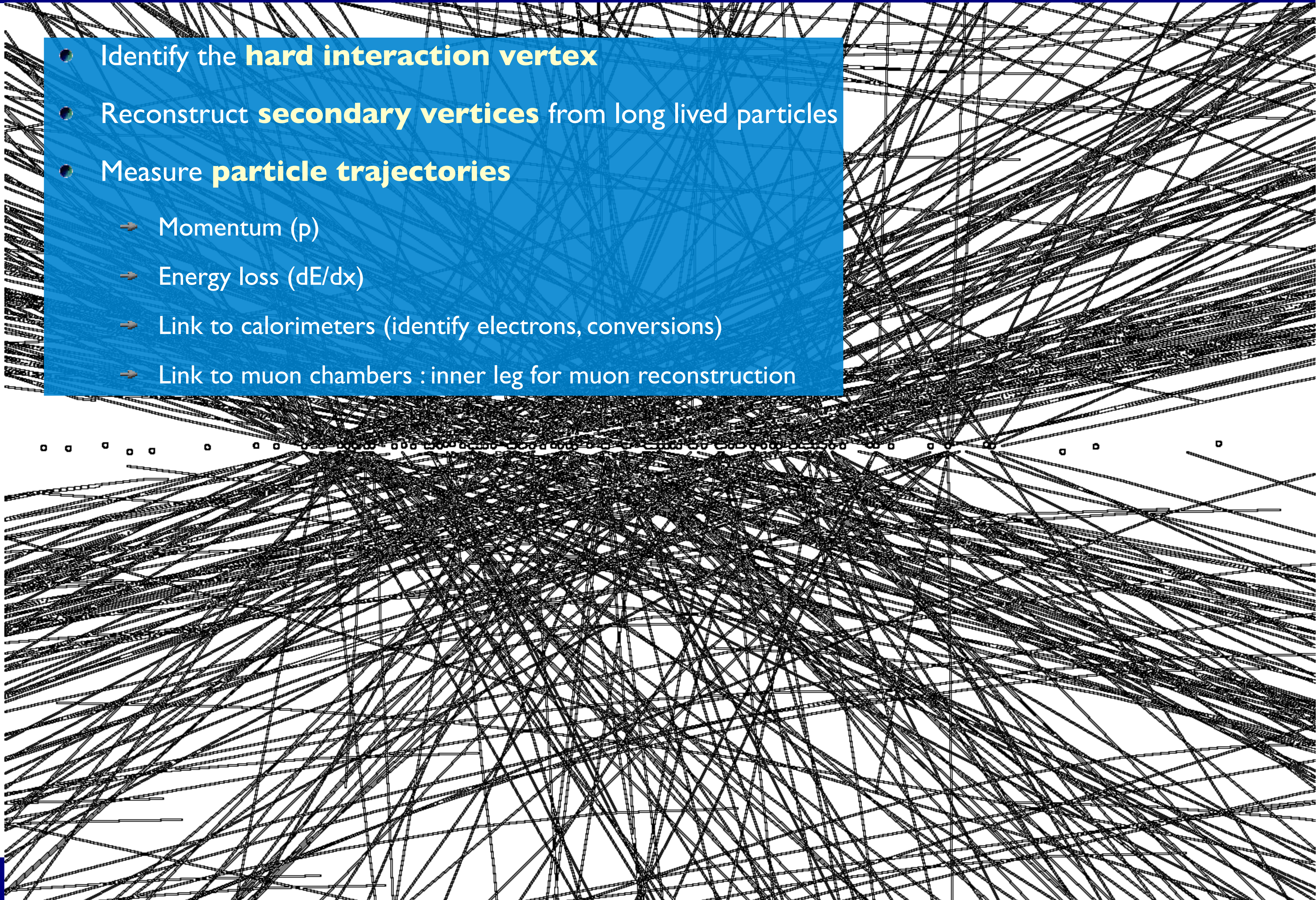

Tracking: why?

- Identify the **hard interaction vertex**
- Reconstruct **secondary vertices** from long lived particles
- Measure **particle trajectories**
  - Momentum (p)
  - Energy loss (dE/dx)
  - Link to calorimeters (identify electrons, conversions)
  - Link to muon chambers : inner leg for muon reconstruction

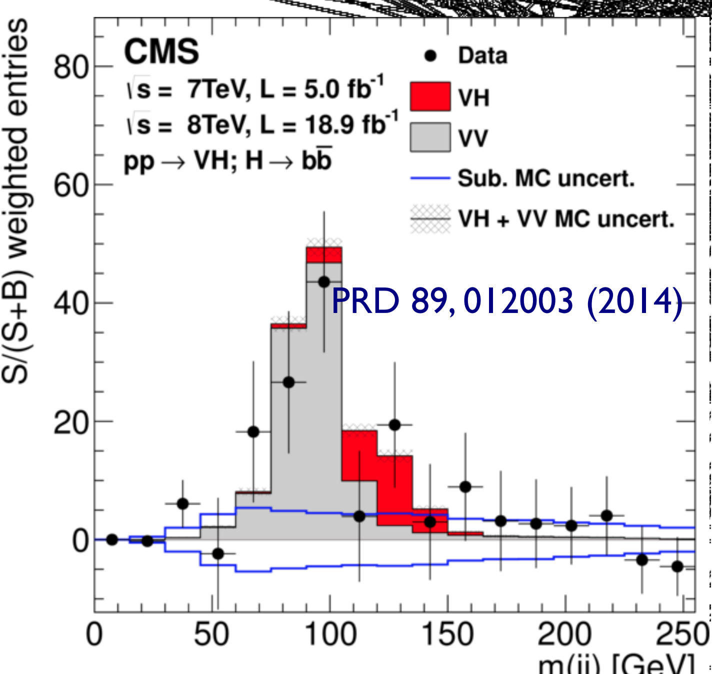

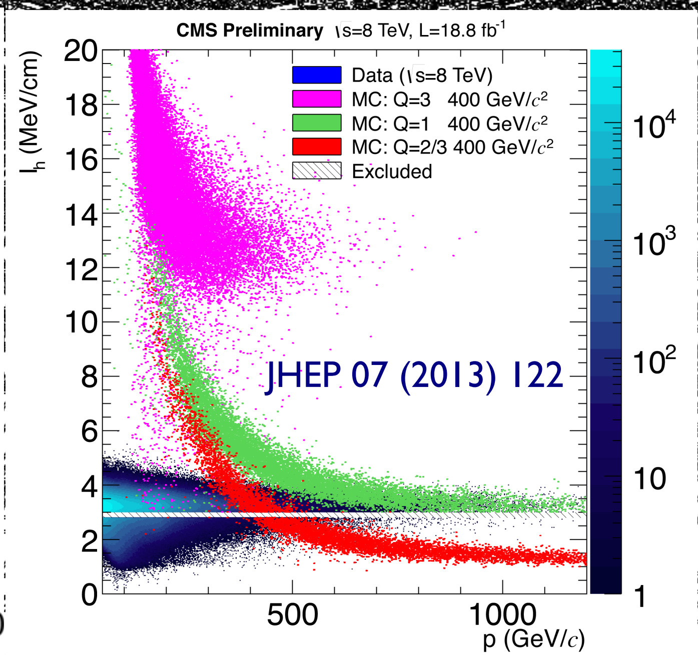

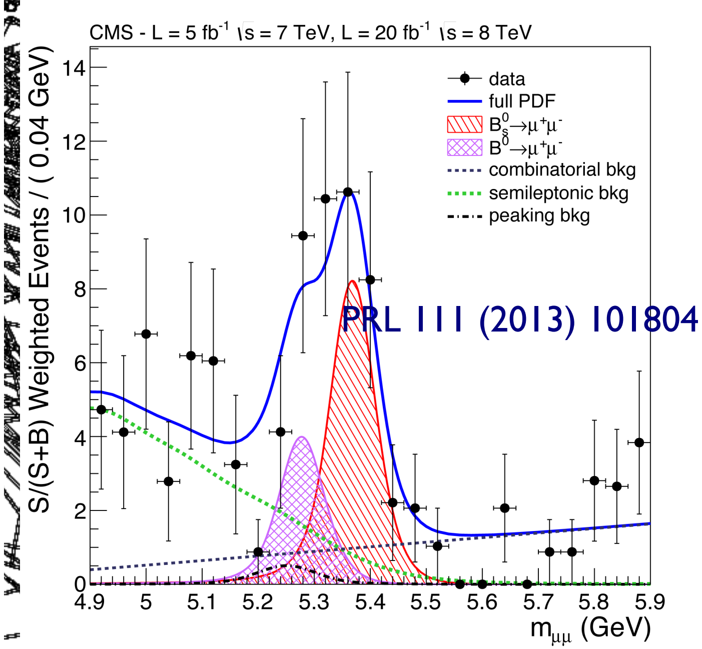

Usage of Si-based trackers for HEP

- **Kemmer, 1979** transferred Si-technology for electrons to detector - NIM 169(1980)499
- **NA11/32** spectrometer at CERN ▶
  - 6 planes Si-Strip, <2k channels
  - Fesolution ~4.5μm

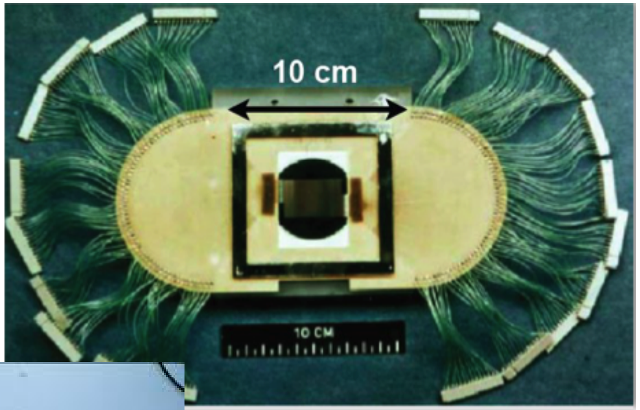

- **ALEPH** detector at LEP ▶
  - Enable precise measurements for B-physics (lifetime, b-tagging)

Experiment	Detectors	Channels (10^3)	Si area [m^2]
Aleph (LEP)	144	95	0.49
CDF II (TEV)	720	405	1.9
D0 II (TEV)	768	793	4.7
AMS II	2300	196	6.5
ATLAS (LHC)	4088	6300	61
CMS (LHC)	15148	10000	200

Inner tracking at the LHC - I

- Resolve 25 ns bunch crossings, keep low occupancy in high pileup regime
- Radiation hard, low material budget in front of calorimeters
- Good momentum resolution, and high efficiency
- Identify b-jets and hadronically decaying τ

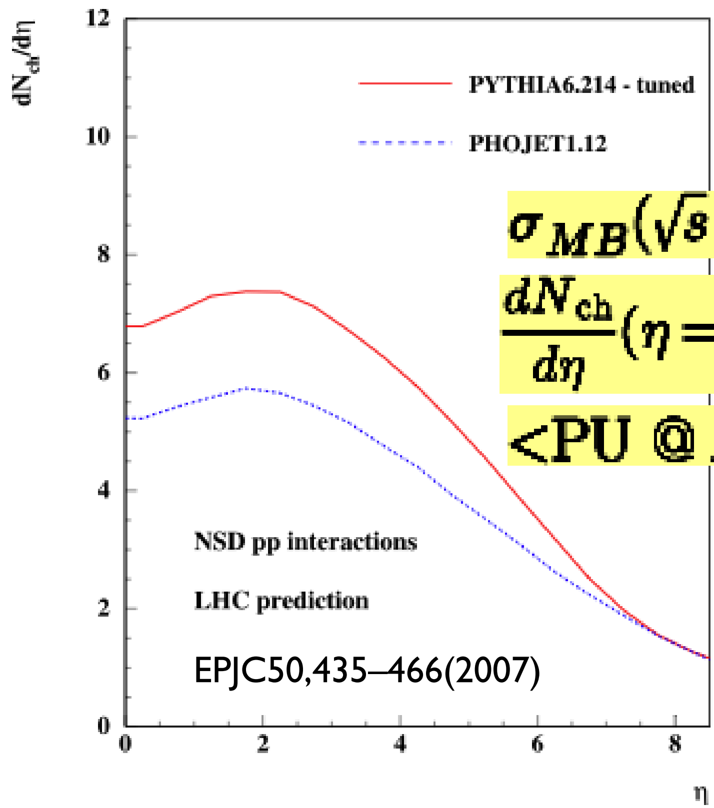

$$\sigma_{MB}(\sqrt{s}=14\text{TeV})\sim 100\text{mb}$$

$$\frac{dN_{\rm ch}}{d\eta}(\eta=0)\sim 7$$

$$<\text{PU} @ \mathcal{L}=10^{34}\text{cm}^{-2}\text{s}^{-1}>\sim 20$$

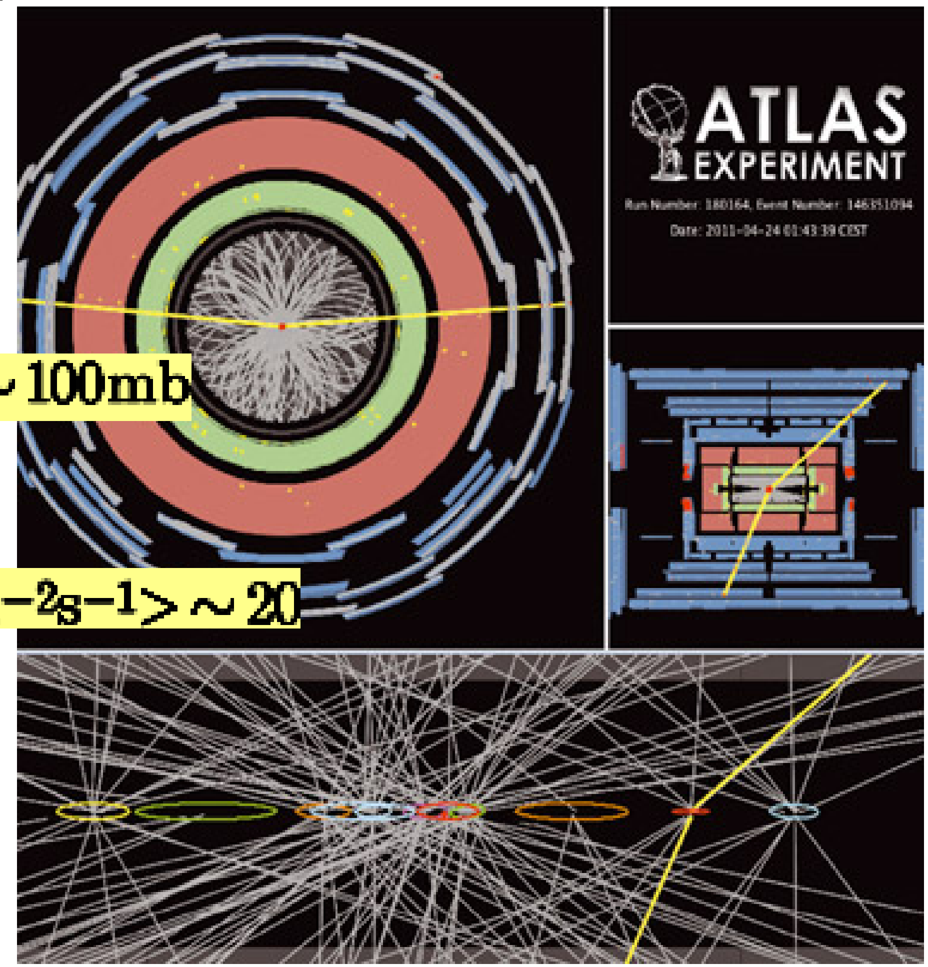

Inner tracking at the LHC - II

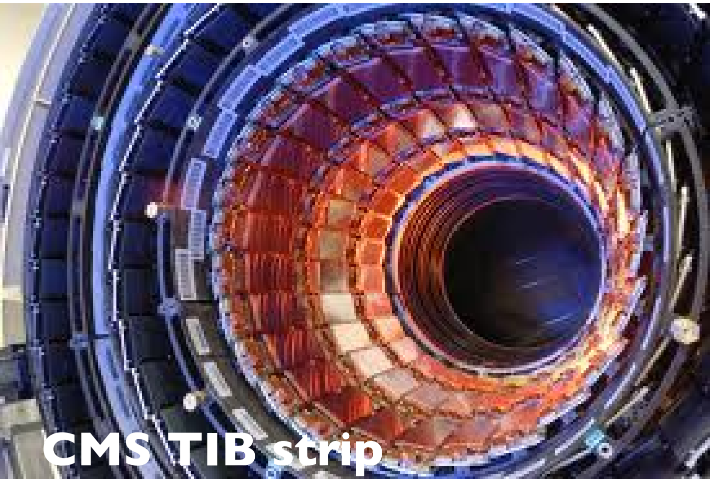

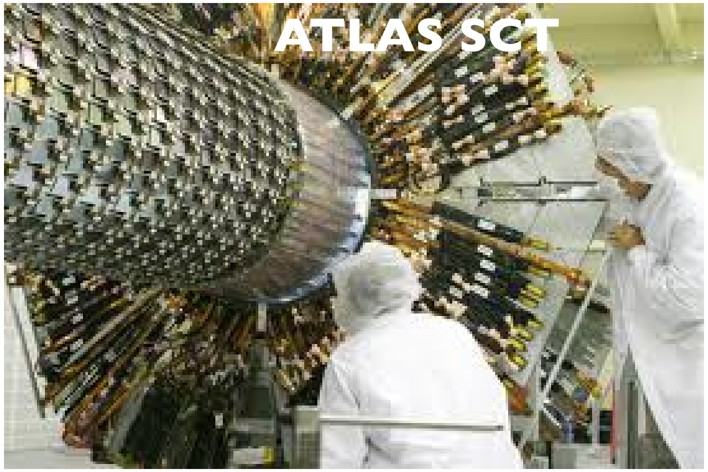

Tracking: what?

- While transversing a medium a **charged particle leaves an ionization trace**
  - create a depletion zone in between electrodes: gaseous, liquid or solid-state (semi-conductor)
  - ionization charges drift towards electrodes
  - amplify electric charge signal and deduce position from signals collected in individual strips

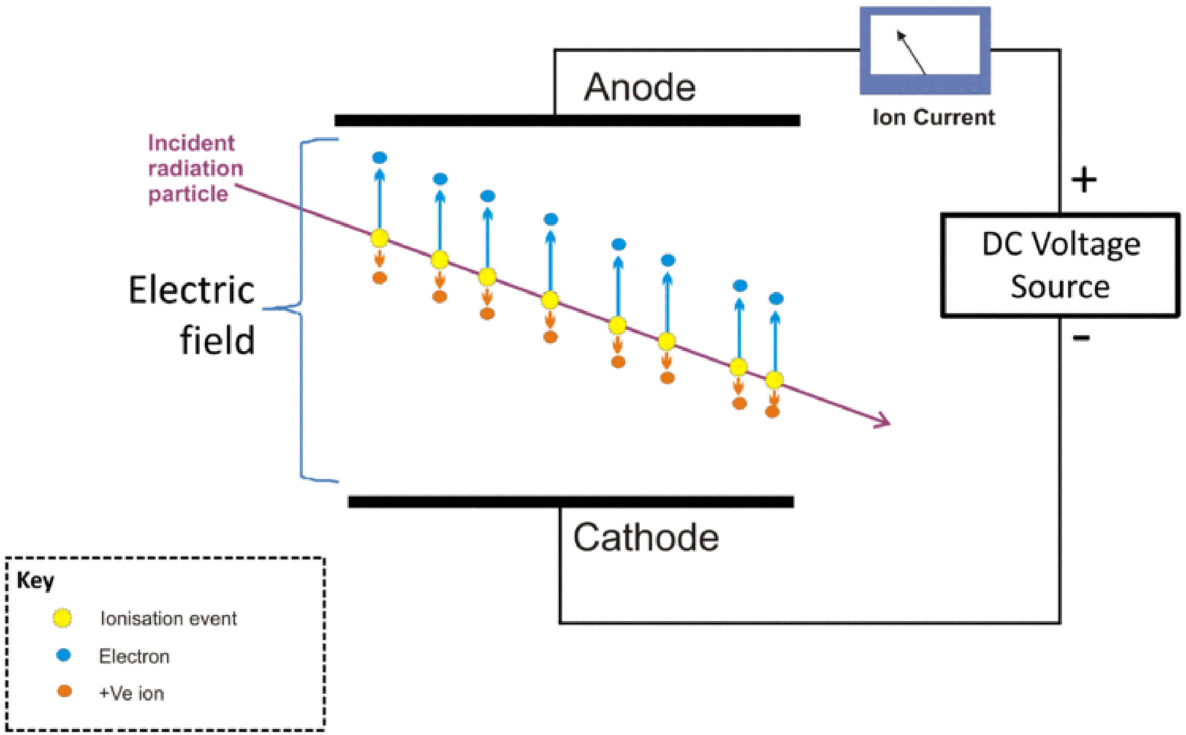

ionization chamber ~ *Si strip detector*

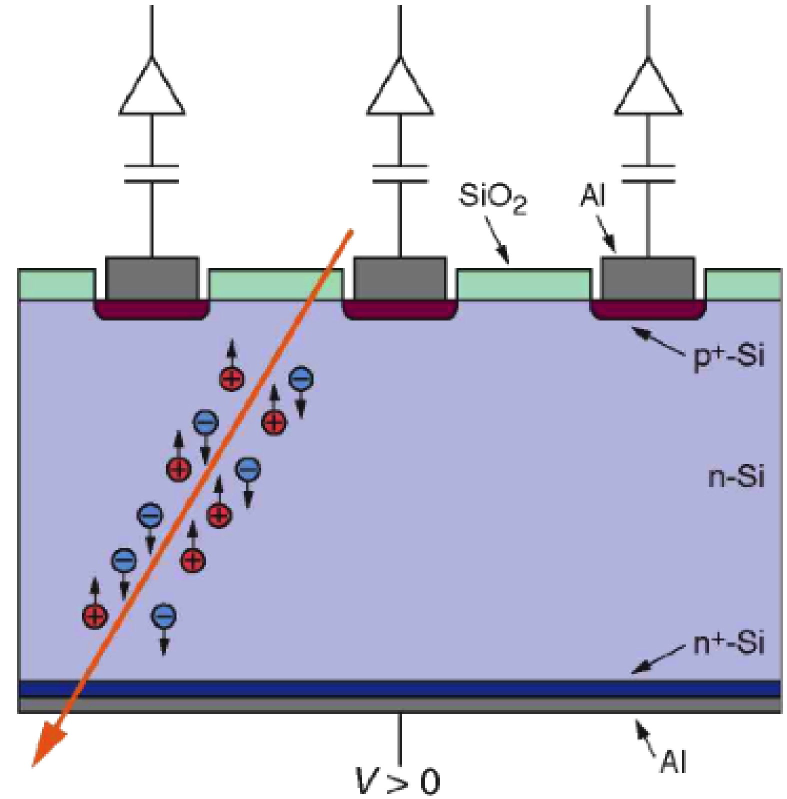

Tracking: how?

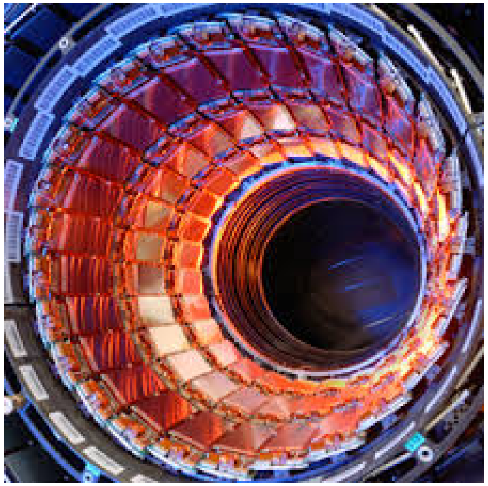

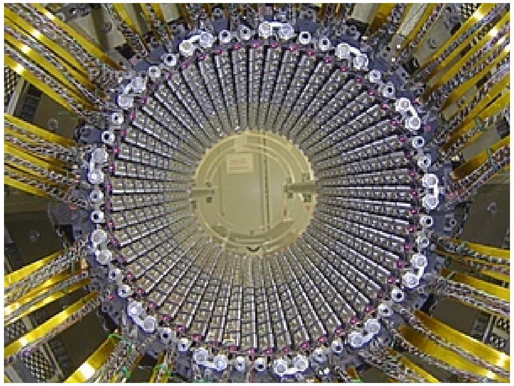

- **Solid state detectors**
  - Ge, Si, Diamond,...
  - Pixels for vertexing, strips for tracking
- **Gaseous detectors**
  - drift tubes, resistive plate chambers, gas electron multipliers, ...
  - usually for outer tracking

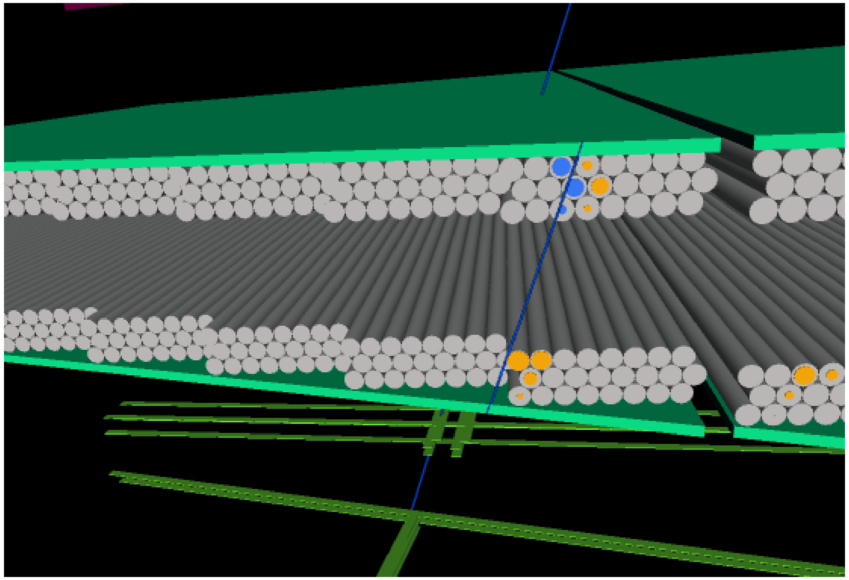

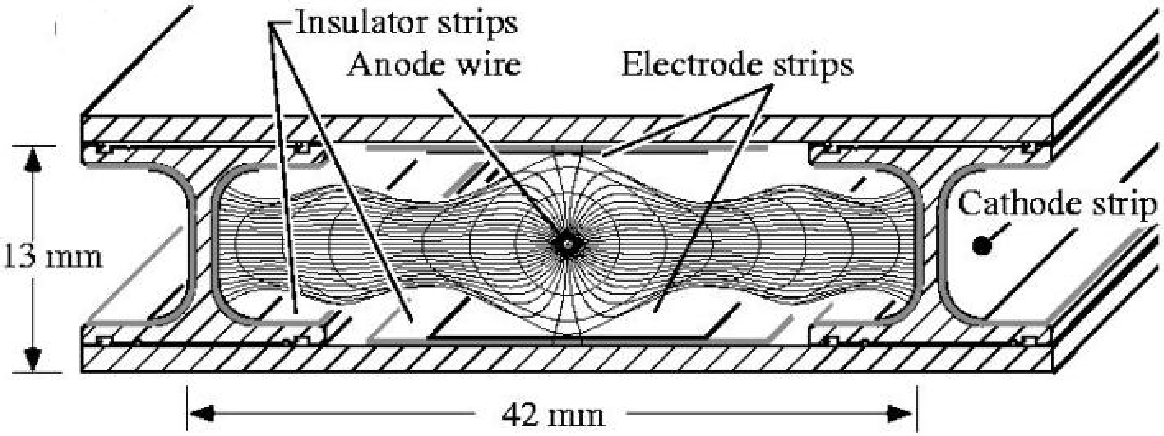

Gaseous versus solid state

	Gas		Solid state	
Density (g/cm³)	Low	$C_2H_2F_4$	High	Si
Atomic number (Z)	Low	(~95% for CMS RPC)	Moderate	
Ionization energy (ε_I)	Moderate	30eV	Low	3.6eV
Signal speed	Moderate	10ns-10μs	Fast	<20ns

- In solid state detectors ionization energy converts in e-h pairs
  - 10 times smaller with respect to gaseous-based ionization
  - Charge is increased → improved E resolution

$$n = \frac{E_{\rm loss}}{E_{\rm eh}} \rightarrow \frac{\sigma_{\rm E}}{\rm E} \propto \frac{1}{\sqrt{n}} \propto \sqrt{E_{\rm eh}}$$

- Higher density materials used in solid state detectors
  - Charge collected is proportional to the thickness
  - Most probable value:

$$\frac{\Delta_p}{x} \sim 0.74 \cdot 3.876 \mathrm{MeV} / \mathrm{cm} \rightarrow N_{eh} \sim \frac{23 \cdot 10^3}{300 \mu m}$$

  - Excellent spatial resolution: short range for secondary electrons

Si properties

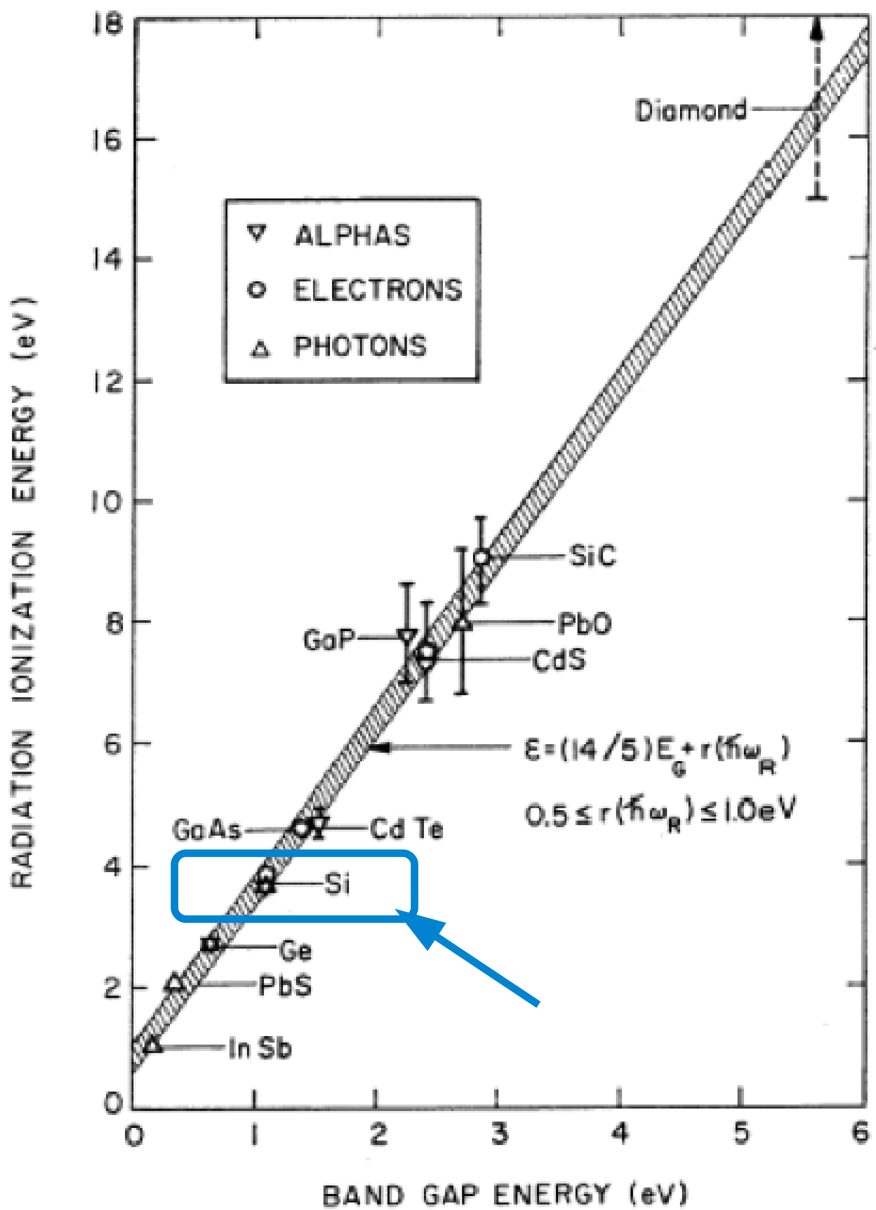

Excellent material for HEP detectors

- **Low ionization energy**
  - Band gap is 1.12 eV
  - Takes 3.6 eV to ionize atom → remaining yields phonon excitations
  - Long free mean path → good charge collection efficiency
  - High mobility → fast charge collection
  - Low Z → reduced multiple scattering
- **Good electrical properties (SiO_2)**
- **Good mechanical properties**
  - Easily patterned to small dimensions
  - Can be operated at room temperature
  - Crystalline → resilient against radiation
- **Widely used in industry**

Bond model of semi-conductors

- **Covalent bonds** formed after sharing electrons in the outermost shell
- **Thermal vibrations**
  - break bonds and yield electron conduction (free e$^-$)
  - remaining open bonds attract free e- → holes change position → hole conduction

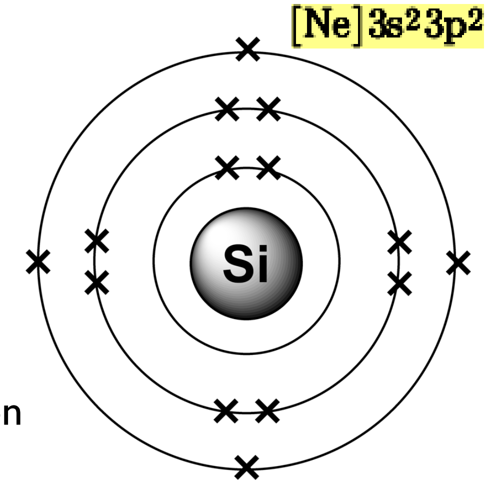

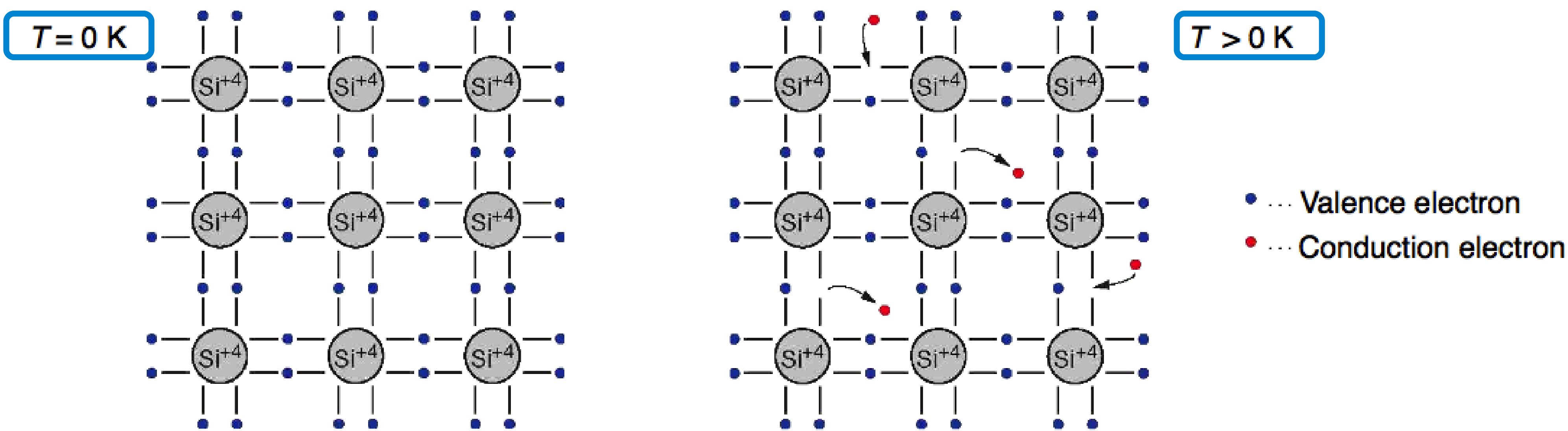

Energy bands

- **In solids, the quantized energy levels merge**
  - Metals: conduction and valence band overlap
  - Insulators and semi-conductors: conduction and valence band separated by energy (band) gap

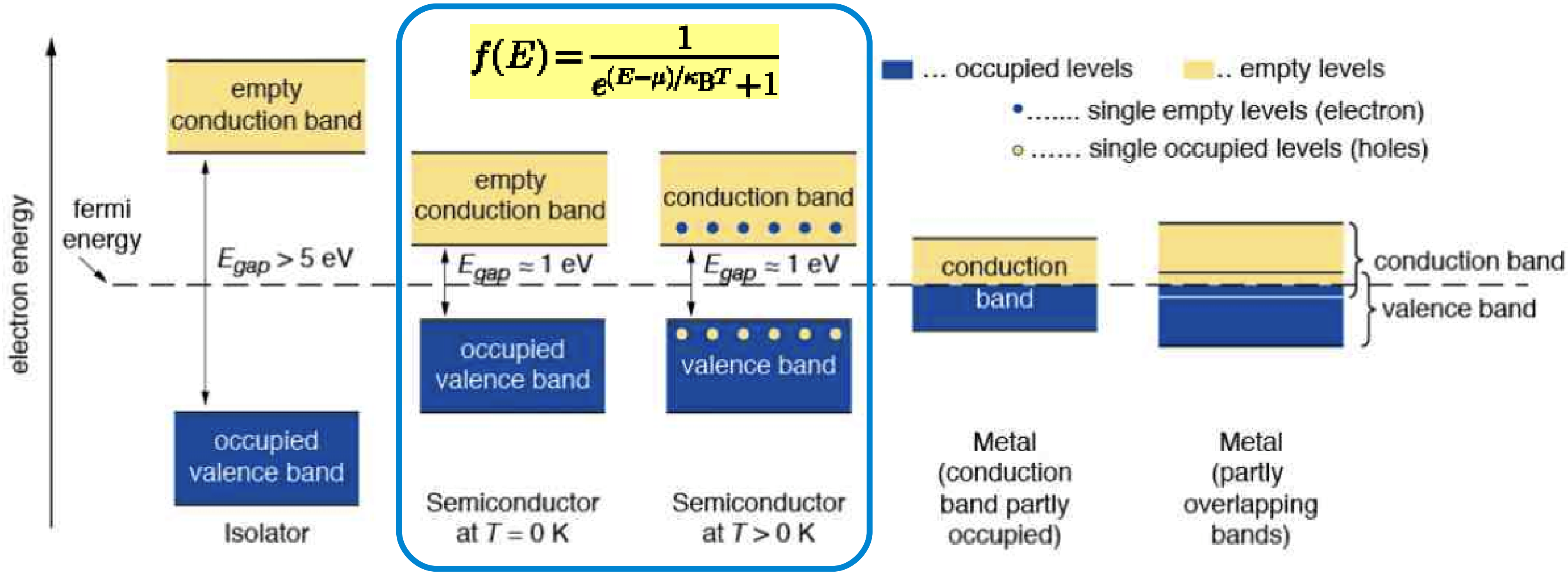

Intrinsic carrier concentration

- The probability that an energy state is occupied by an e^- is given by **Fermi statistics** ▼
- **At room temperature**
  - excited electrons occupy conduction band
  - electrons tend to recombine with holes
- **Excitation** and **recombination in thermal equilibrium**
  - Intrinsic carrier concentration given by

    $$n_e = n_h = n_i = A \cdot T^{3/2} \cdot e^{-E_g/k_B T}$$

    with $A=3.1\times10^{16}\ K^{-3/2}cm^{-3}$ and $E_g/2k_B=7\times10^3 K$
  - $n_i \sim 1.45\times10^{10}\ cm^{-3} \rightarrow 1/10^{12}$ Si atoms is ionized

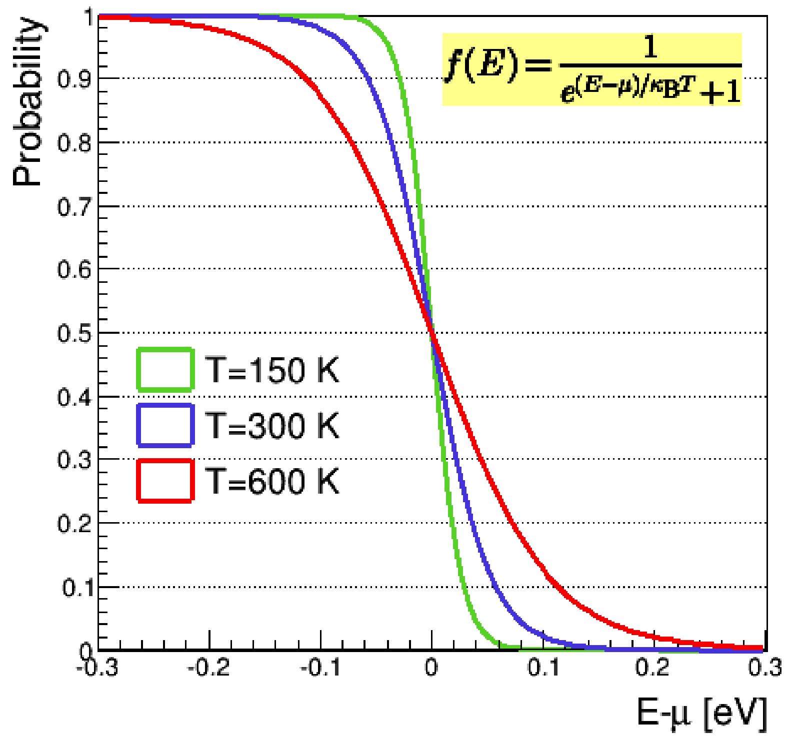

- **Conclusion: S/N in semi-conductors is compromised by the band gap**
  - Keep low ionization energy → small band gap
  - Keep low intrinsic charge carriers → large band gap
  - Optimal $E_g \sim 6$ eV → diamond!

S/R in intrinsic Si detector

$$\left\langle -\frac{dE}{dx}\right\rangle = K z^2 \frac{Z}{A}\frac{1}{\beta^2}\left[\frac{1}{2}\ln\frac{2m_e c^2\beta^2\gamma^2 W_{max}}{I^2} - \beta^2 - \frac{\delta(\beta\gamma)}{2}\right]$$

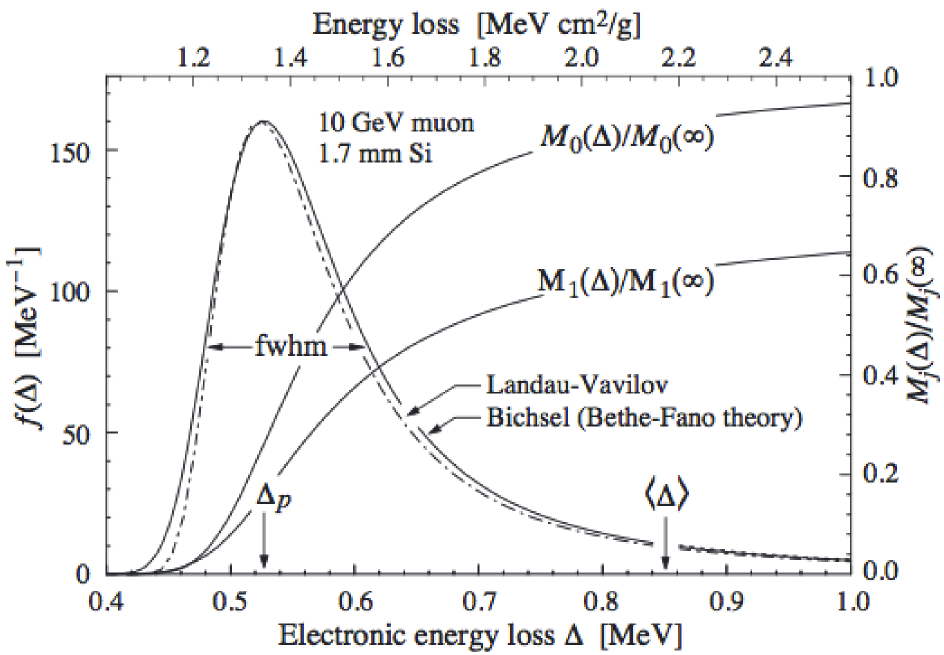

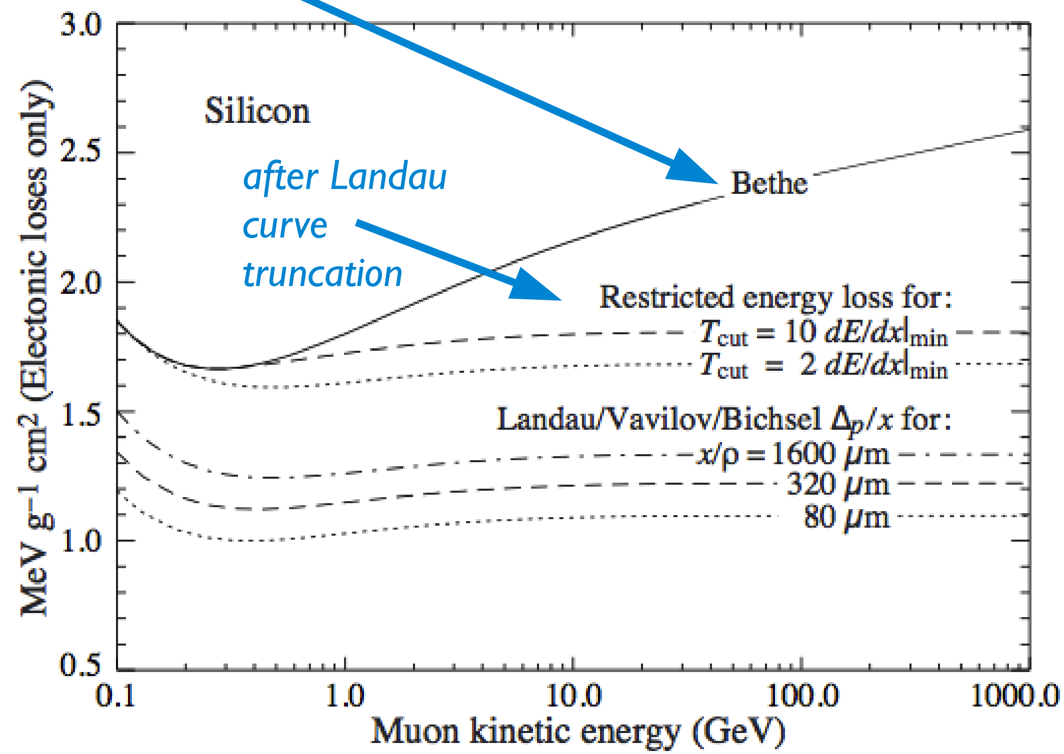

- E.g. consider a Si detector with thickness d=300μm
  - Minimum ionizing particle (MIP) creates: $\frac{1}{E_{eh}}\frac{dE}{dx}\cdot d = \frac{3.87\cdot 10^6 \mathrm{eV/cm}}{3.63\mathrm{eV}}\cdot 0.03\mathrm{cm} = 3.2\cdot 10^4 \text{eh pairs}$
  - Intrinsic charge carriers (per cm²): $n_i \cdot d = 1.45\cdot 10^{10} cm^{-3}\cdot 0.03 cm = 4.35\cdot 10^8 \text{eh pairs}$
- **Number of thermally-created e-h pairs exceeds mip signal by factor 10!**
  - Depletion of free charge carriers needed!

Si doping: n-dope bond model

- Doping with a group 5 atom (e.g. P, As, Sb)
  - Doping atom is an electron **donor/donator**
  - Weakly bound 5th valence electron
  - Positive ion is left after conduction electron is released

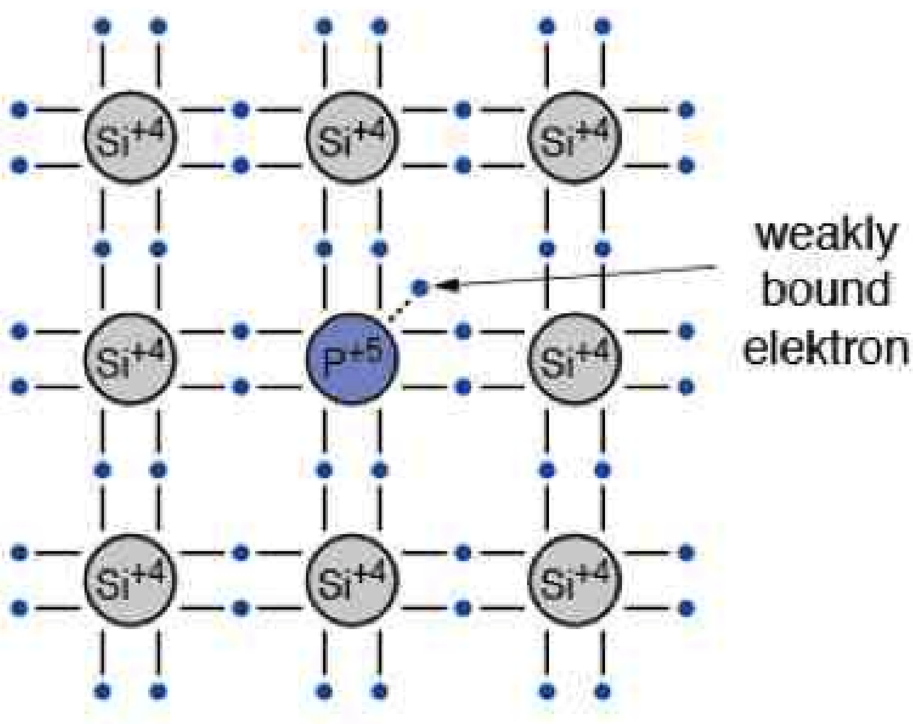

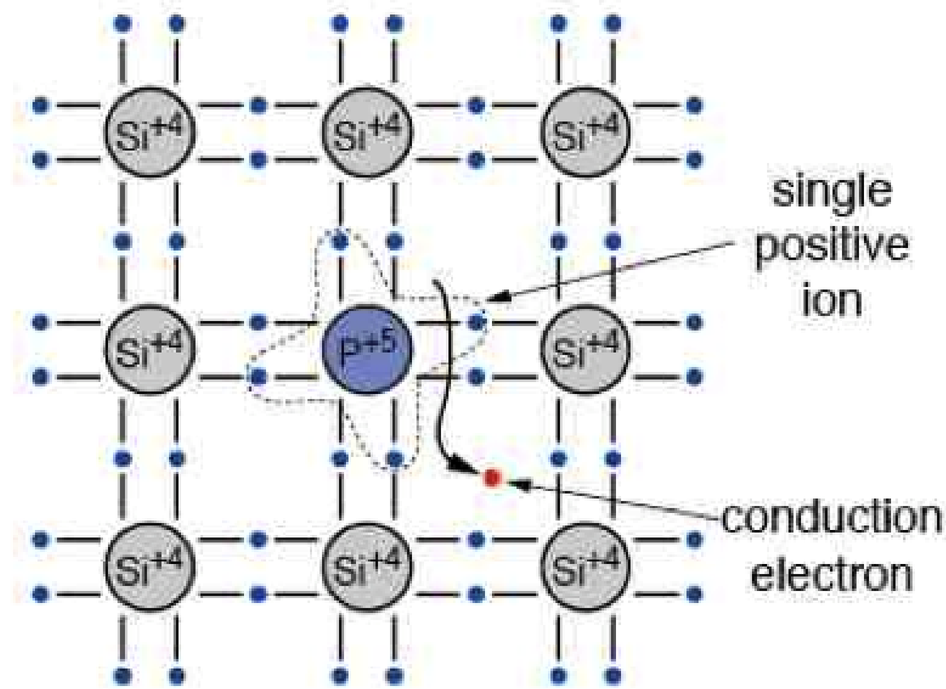

Si doping: n-dope bond model II

- Energy level of donor is below edge of conduction band
  - Most electrons enter conduction band at room temperature
  - Fermi level moves up with respect to pure Si

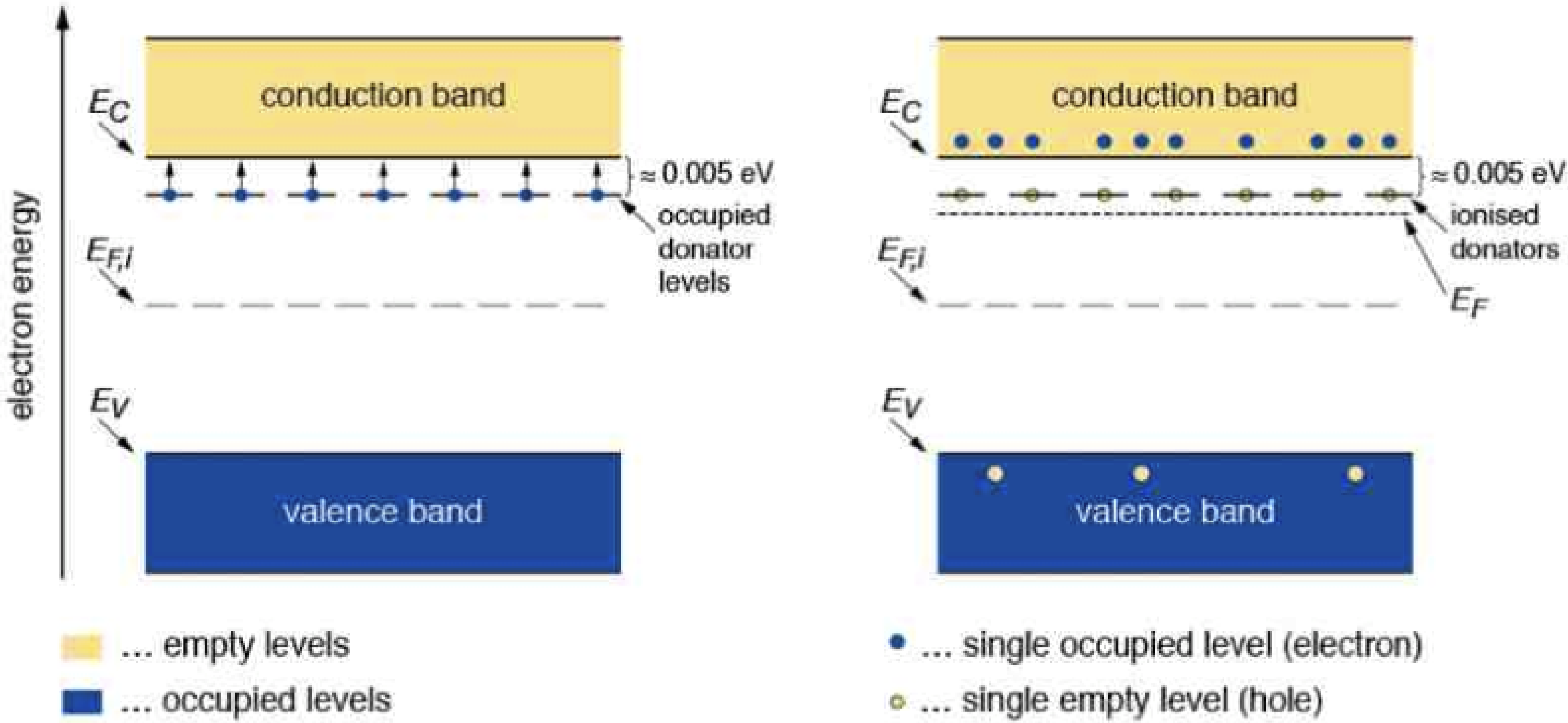

Si doping: p-dope bond model

- Doping with a group 3 atom (e.g. B, Al, Ga, In)
  - Doping atom is an electron **acceptor**
  - Open bond attracts electrons from neighboring atoms
  - Acceptor atom in the lattice becomes negatively charged

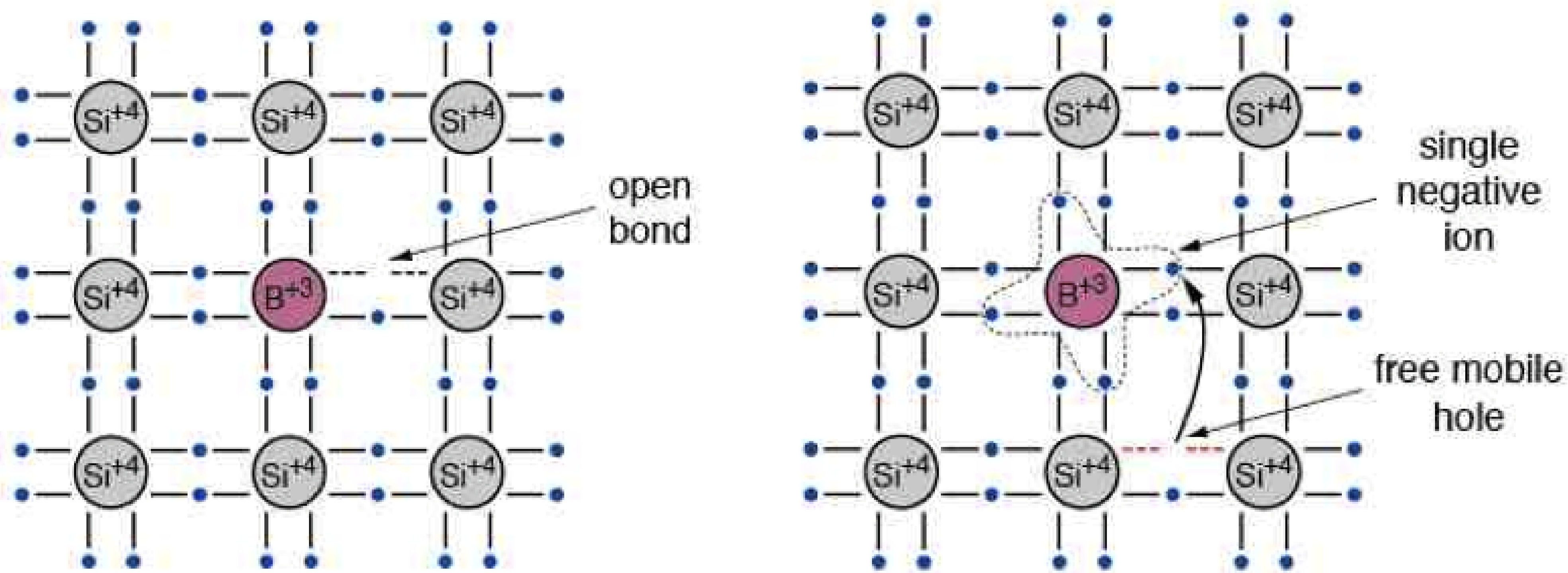

Si doping: p-dope bond model - II

- Energy level of acceptor is above edge of conduction band
  - Most levels are occupied by electrons → holes in the valence band
  - Fermi level moves down with respect to pure Si

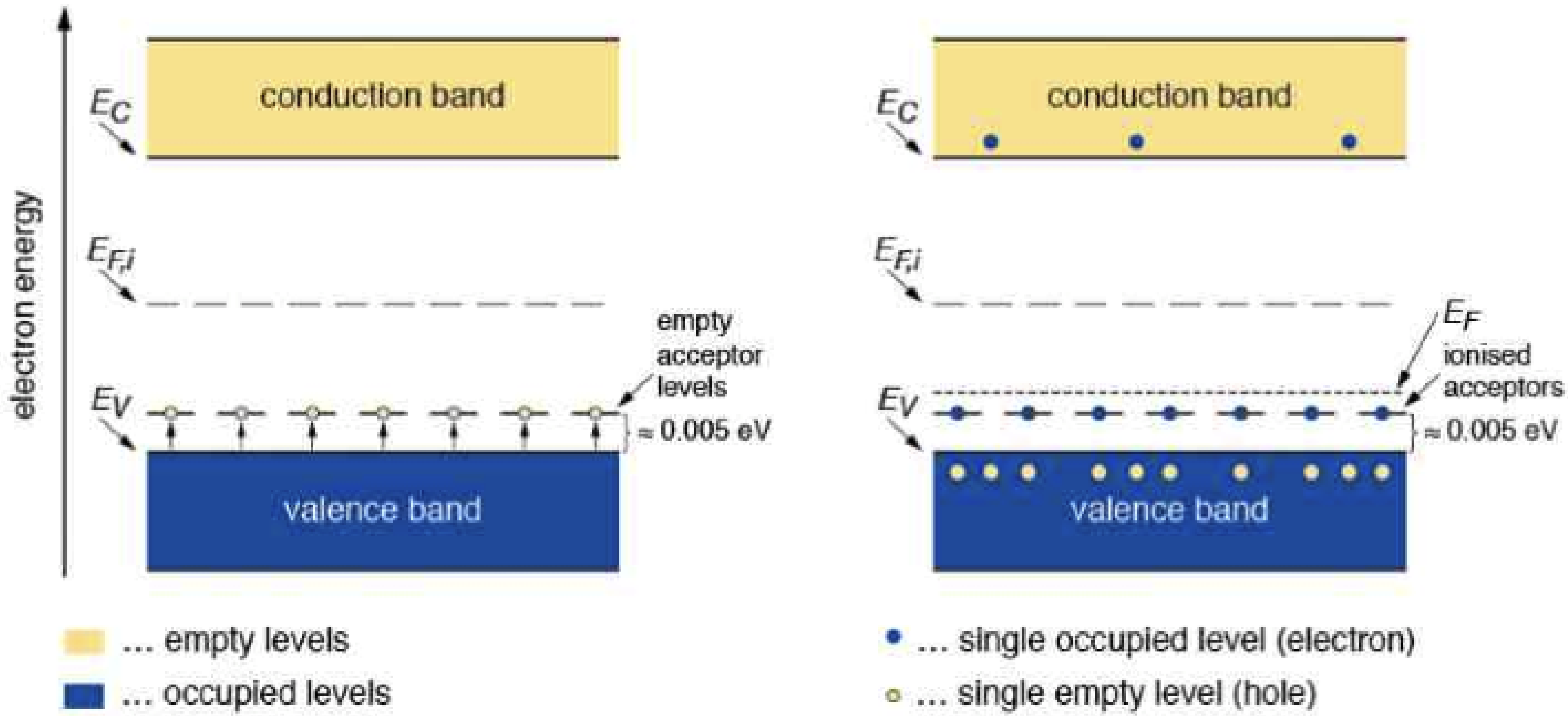

p-n junctions

- Difference in Fermi levels at the interface of n-type or p-type
  - diffusion of excess of charge carriers until thermal equilibrium (or equal Fermi level)
  - remaining ions create a **depletion zone**: electric field prevents further the diffusion

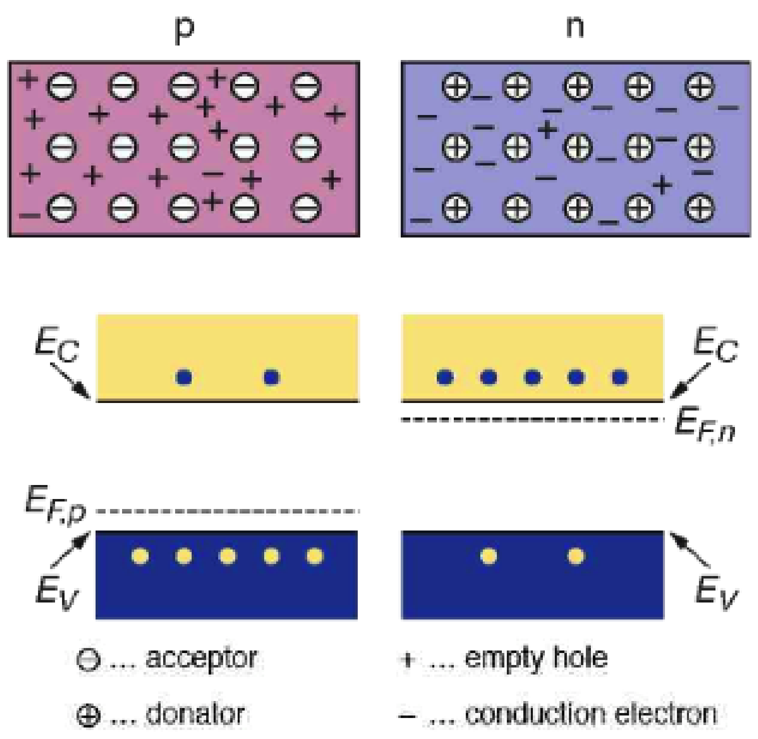

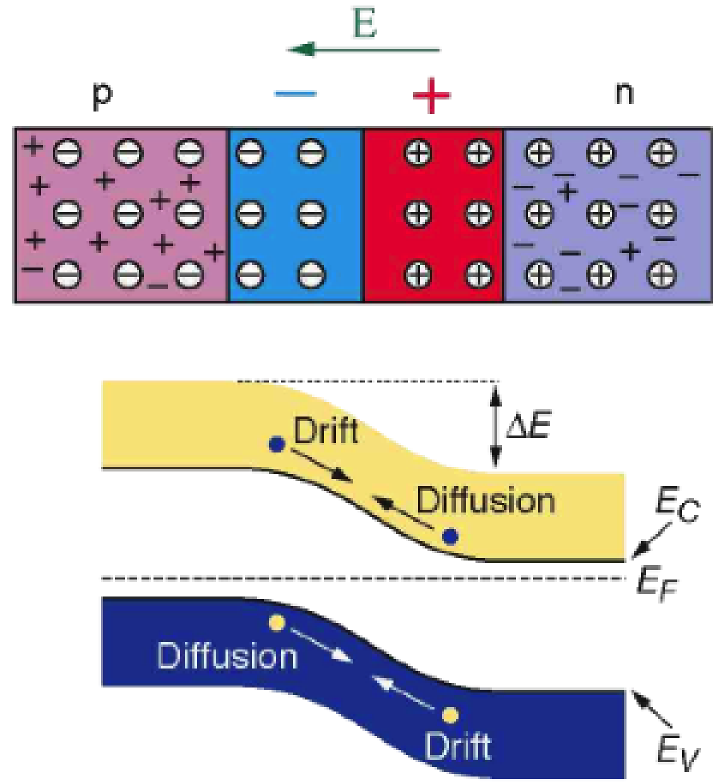

p-n junctions

pn junction scheme

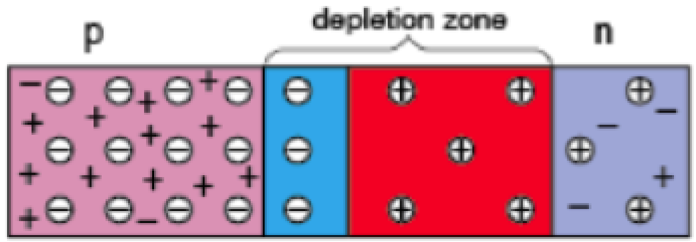

concentration of free charge carriers

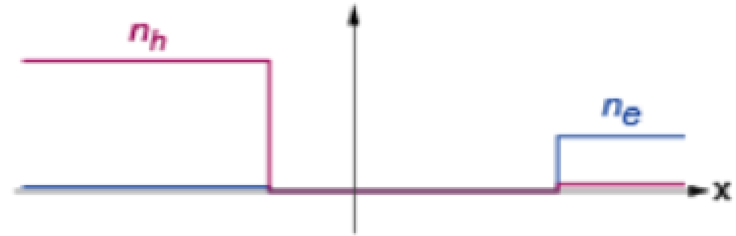

acceptor and donator concentration

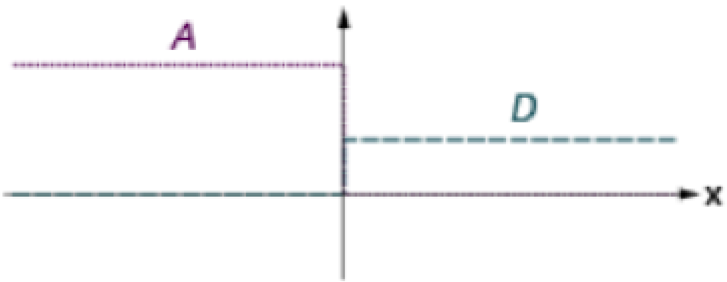

electric field

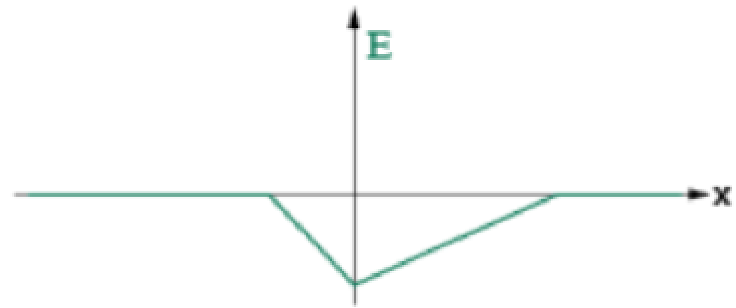

space charge density

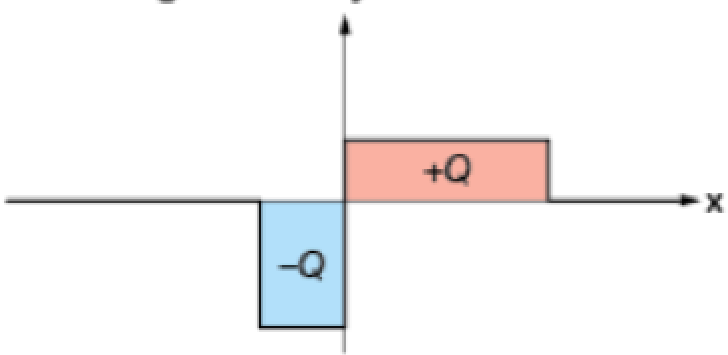

electric potential

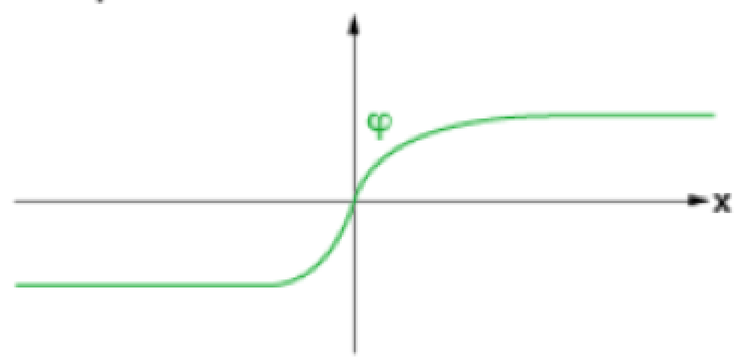

⊖ ... acceptor

+ ... empty hole

⊕ ... donator

− ... conduction electron

Biasing p-n junctions

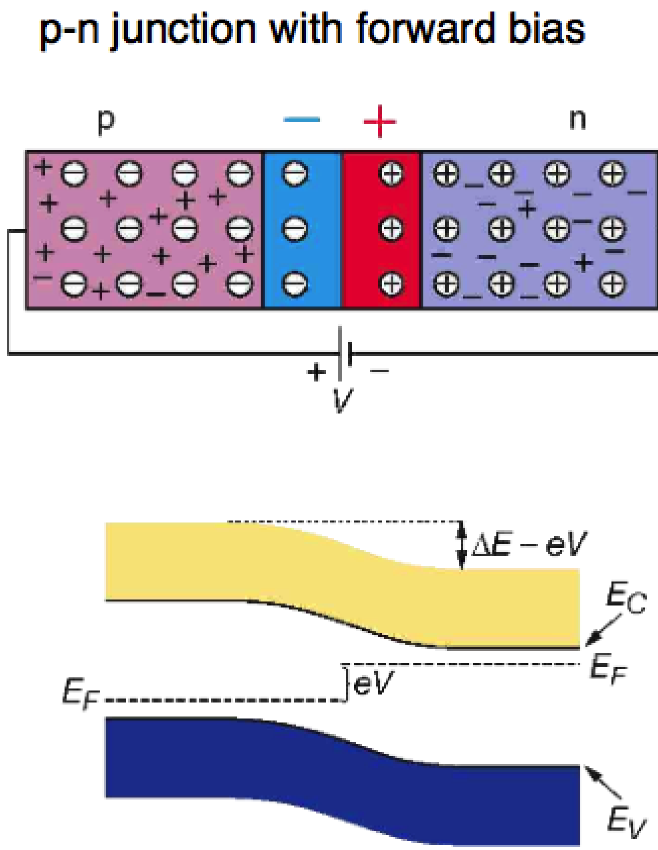

Forward-biased junction

- Anode to p, cathode to n
- Depletion zone becomes narrower
- Smaller potential barrier facilitates diffusion
- Current across the junction tends to increase

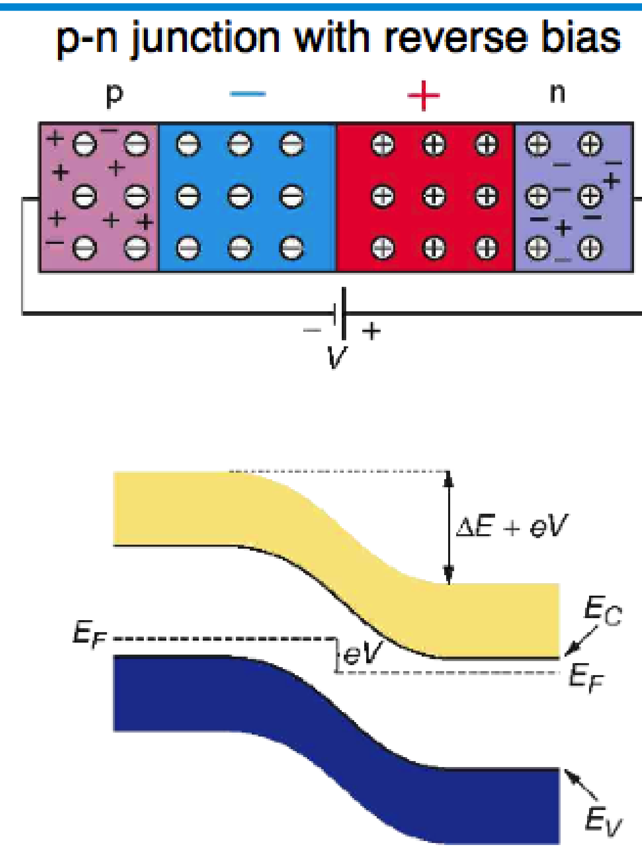

Reverse-biased junction

- Anode to n, cathode to p
- e,h pulled out of the depletion zone
- Potential barrier is suppressed
- Only **leakage current** across junction

Depletion zone width and capacitance

- Characterize depletion zone from Poisson equation with charge conservation: $\nabla^2\phi = -\frac{\rho_f}{\varepsilon}$
- Typically: $N_a=10^{15}$ cm^{-3} (p+ region) >> $N_d=10^{12}$cm^{-3} (n bulk)
- **Width of depletion zone** (n bulk): $W \approx \sqrt{\frac{2\varepsilon V_{\text{bias}}}{q}\cdot\frac{1}{N_d}}$

Reverse bias voltage (V)	W_p (μm)	W_n (μm)
0	0.02	23
100	0.4	363

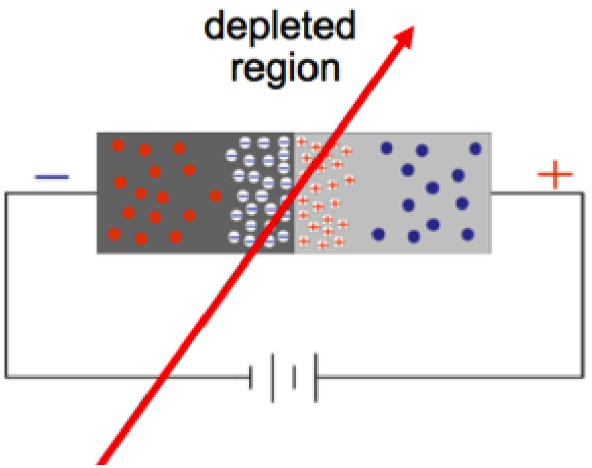

- **Device is similar to a parallel-plate capacitor**

$$C = \frac{q}{V} = \frac{\varepsilon A}{d} = A\sqrt{\frac{\varepsilon q N_d}{2V_{\text{bias}}}}$$

  - Depletion voltage saturates the capacitance
  - Typical curve obtained for CMS strip detector

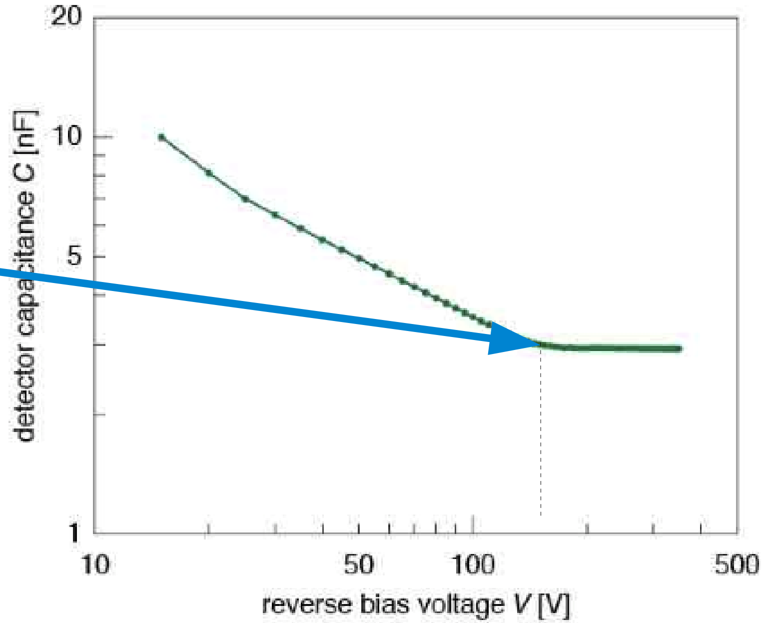

Leakage current

- Thermal excitation generates eh pairs
- Reverse bias applied separates pairs
- eh pairs do not recombine and drift

  → leads to **leakage current**

  Leakage current at room temperature for the CMS strip detector ▼

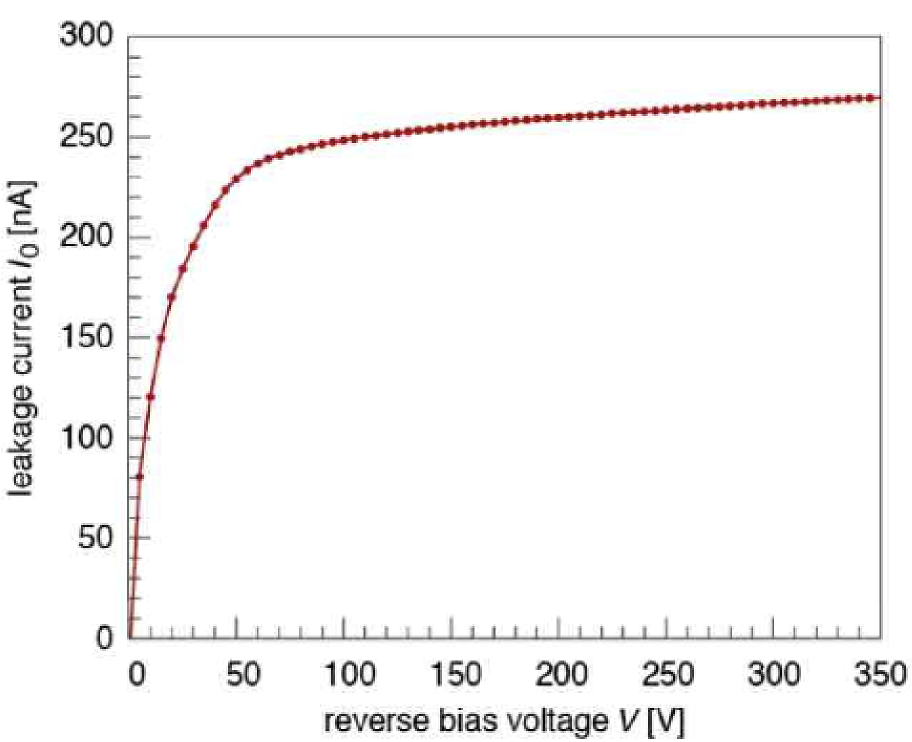

- Depends on purity and defects in material
- Depends on the temperature:

$$j_{\text{gen}} \propto T^{3/2} e^{\frac{1}{\kappa_B T}}$$

  - prefer low, stable temperatures
  - CMS tracker operated at <-10°C

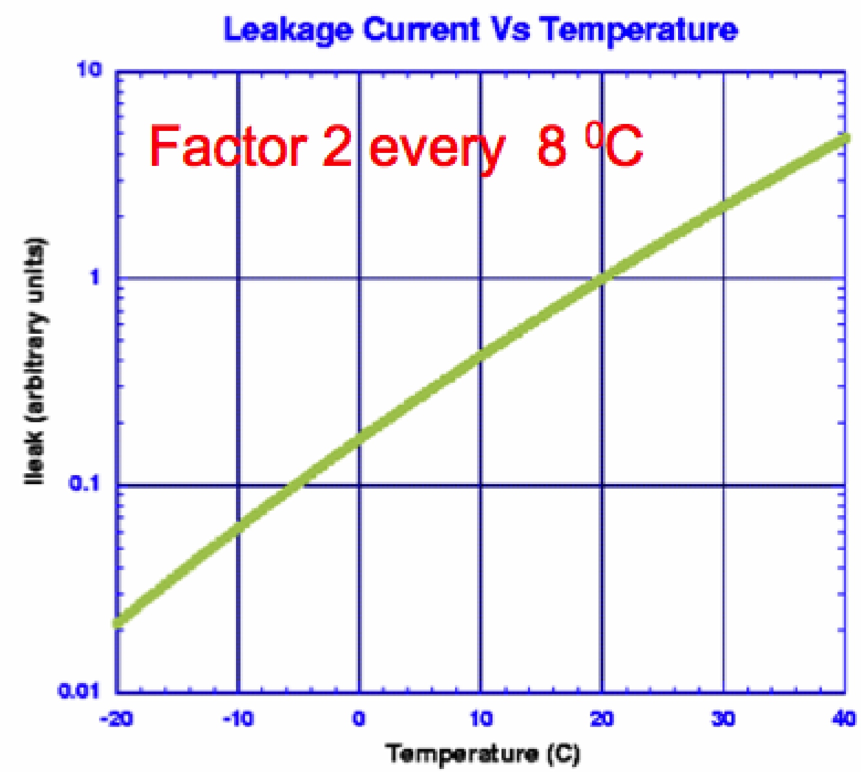

Charge collection

- eh pairs move under the E field
- **Collection time**: time required for a carrier transverse sensitive volume ▶
- Can be reduced over-biasing the sensor
- Simulation of E-field from charge collection after passage of ionizing particle at 45° ▼

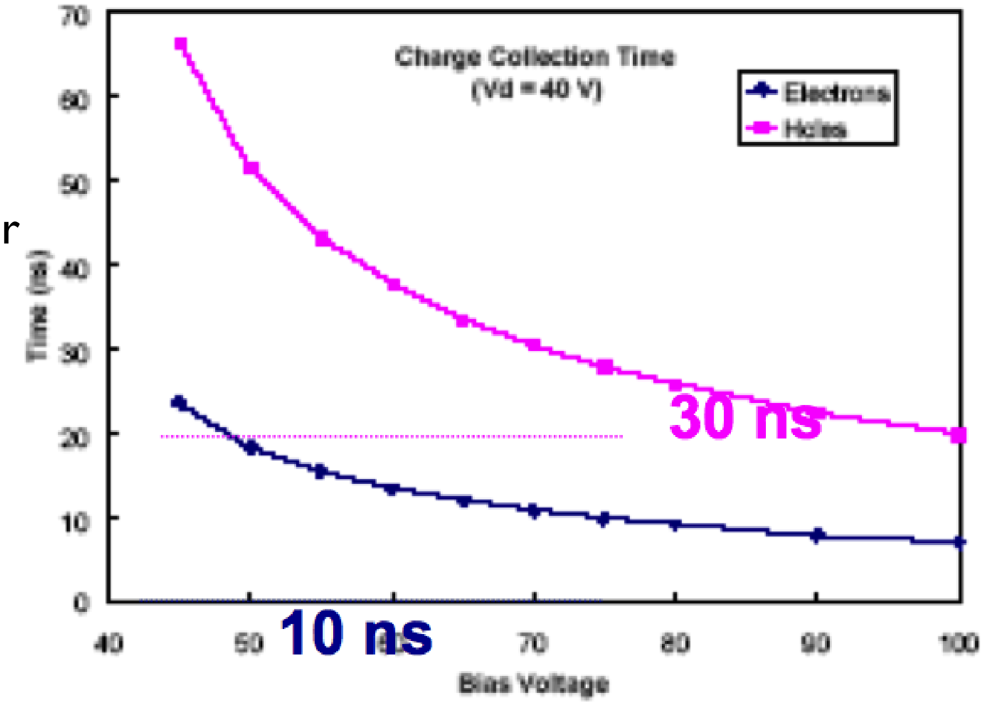

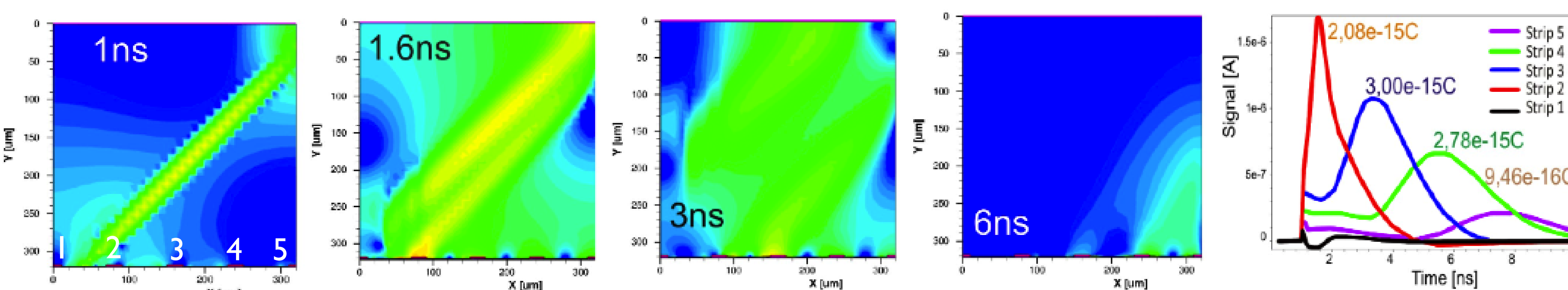

Simulation by Thomas Eichhorn (KIT)

➔ 400 V bias, at 20°C, all charge collected after 10ns

Position resolution (DC coupled)

- Segmentation of the implants
  - reconstruct position of the particle
- Standard configuration uses
  - p implants in strips
  - n-doped substract ~300μm (2-10kΩcm)
  - depletion voltage <200 V
  - Backside P implant establishes ohmic contact and prevents early breakdown
  - Al metallization
- Field closest to the collecting electrodes where most of the signal is induced

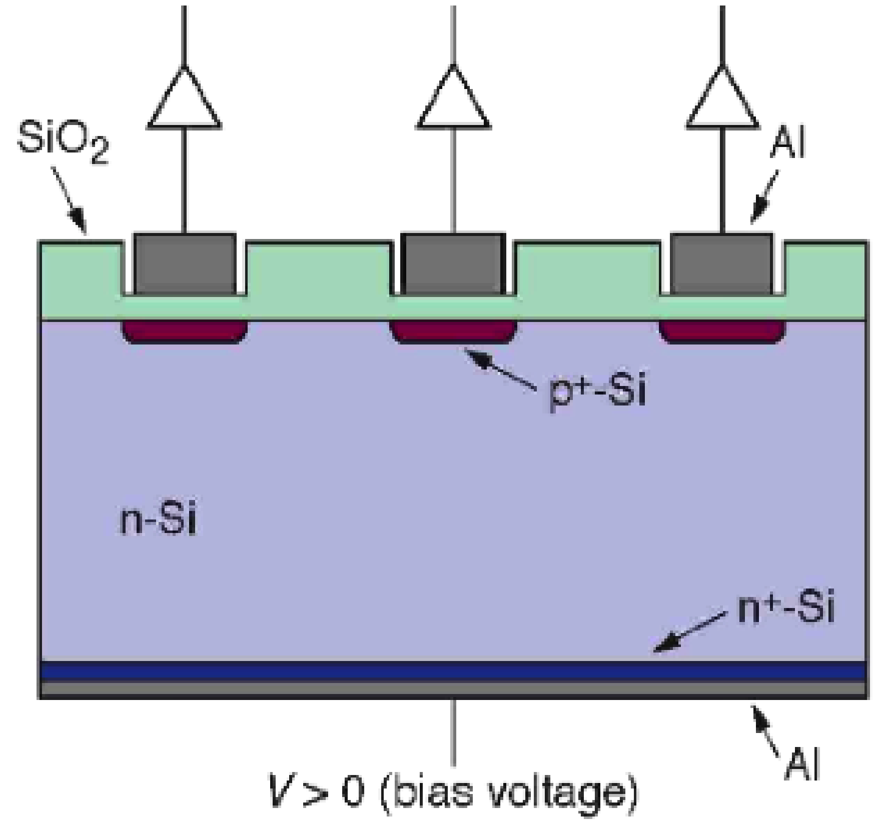

Position resolution (AC coupled)

- **Amplifier generates leakage current**
  - Blocked with AC coupling
- Deposit SiO_2 between p^+ and Al strip
  - Capacitance ~32 pF/cm
  - Shorts through pinholes may be reduced with a second layer of Si_3N_4
- Use large poly silicon resistor (R>1MΩ) connecting the bias voltages to the strips

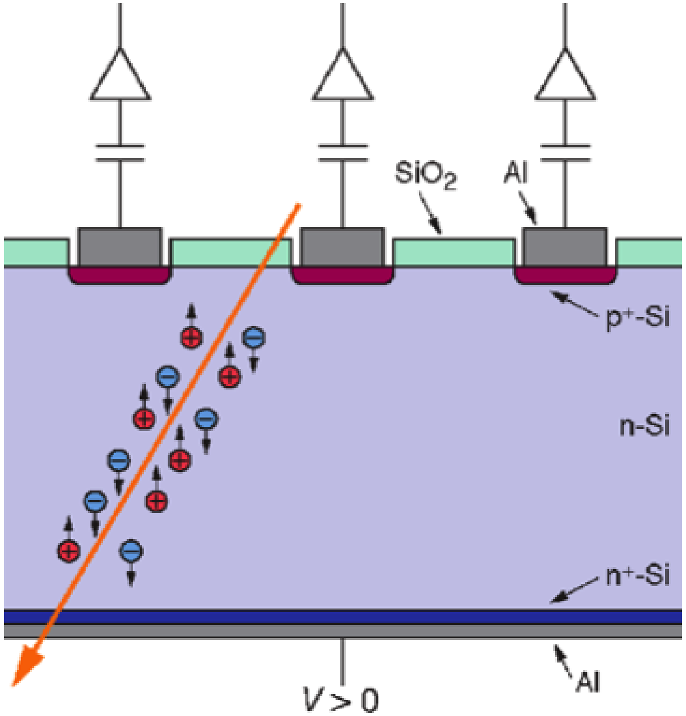

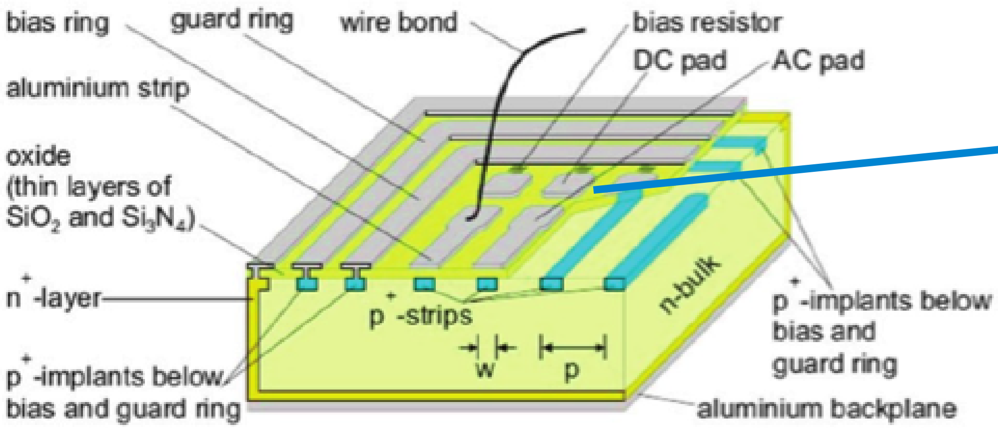

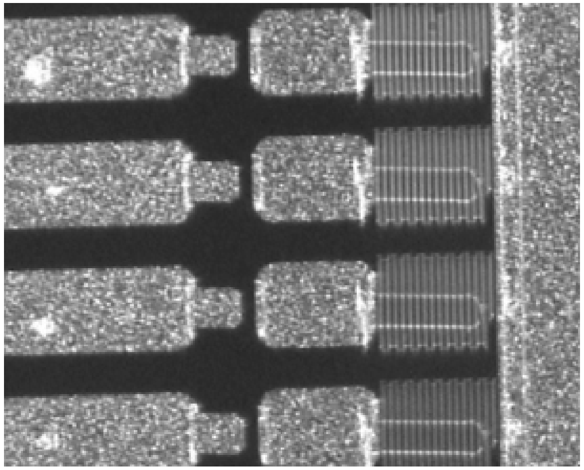

CMS module

silicon sensors
~20 cm strip length

carbon fibre
support

pitch adapter

hybrid
front-end electronics
with read-out chips

kapton flat cables
for power and data

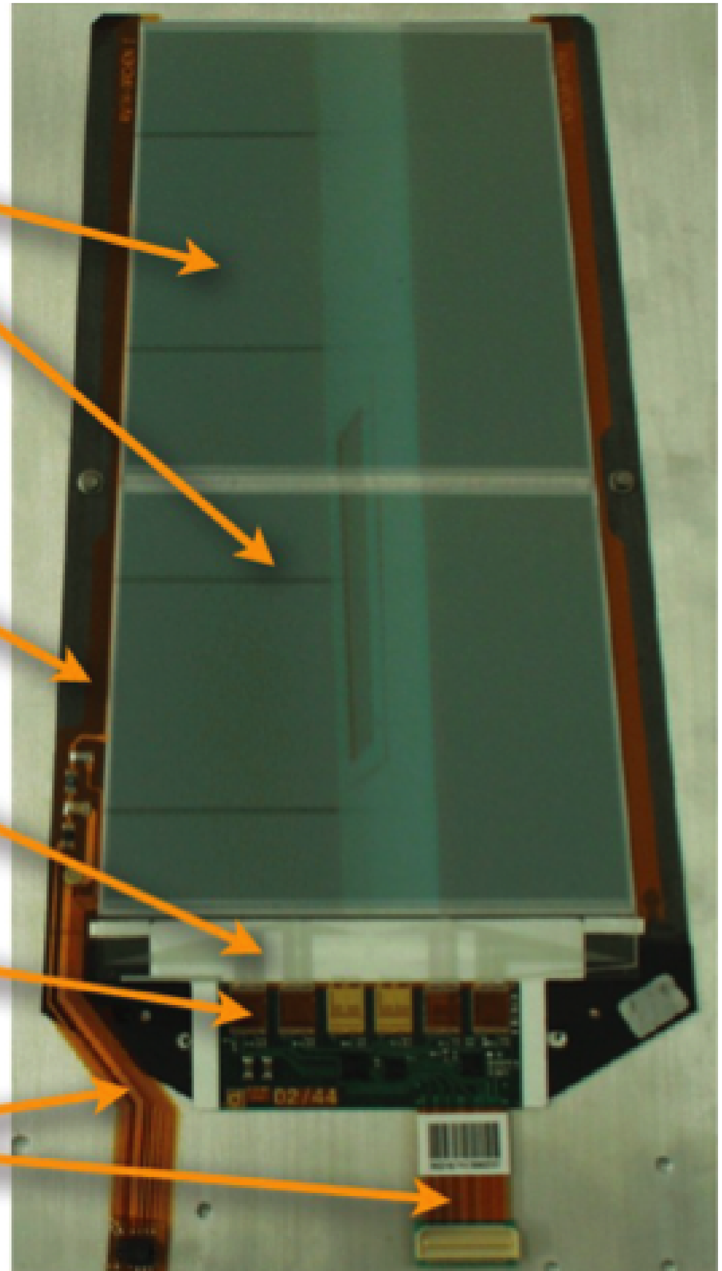

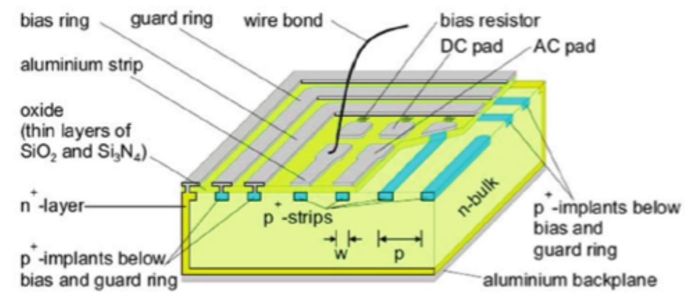

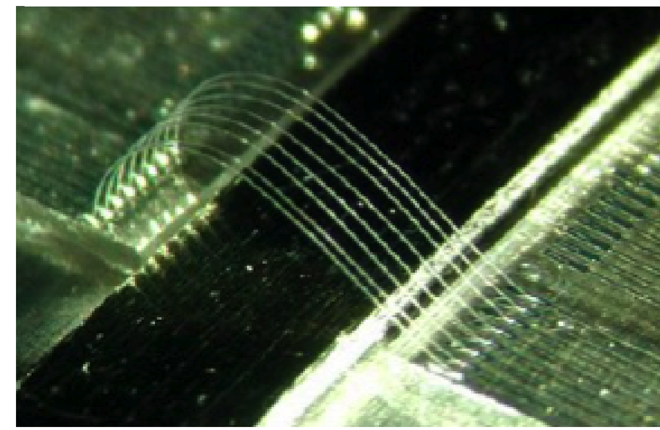

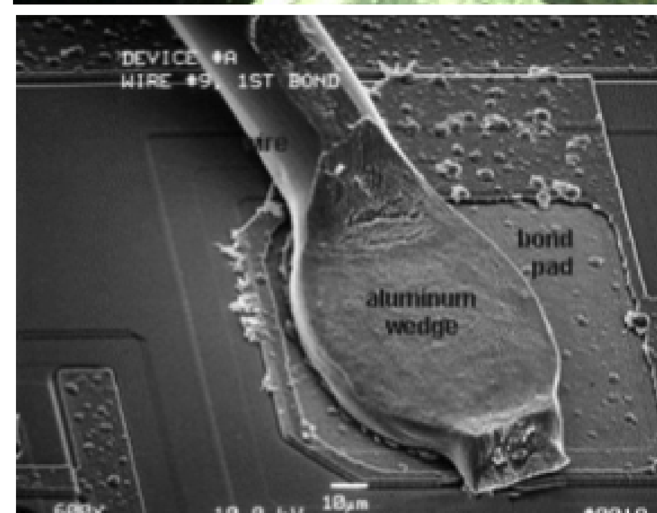

Pixel sensors

- High track density better resolved with 2D position information
  - back-to-back strips for 2D position information → yields "ghost" hits
- **Hybrid pixel detectors** with sensors and readout chips bump-bonded together in model
  - e.g. one sensor, 16 front-end chips and 1 master controller chip

bump-bond

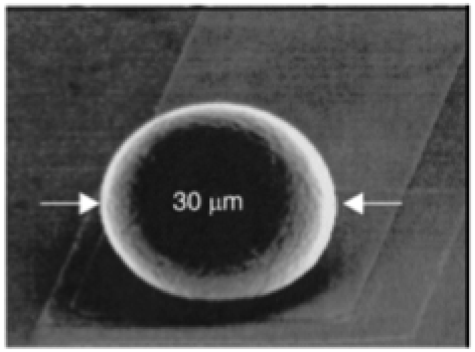

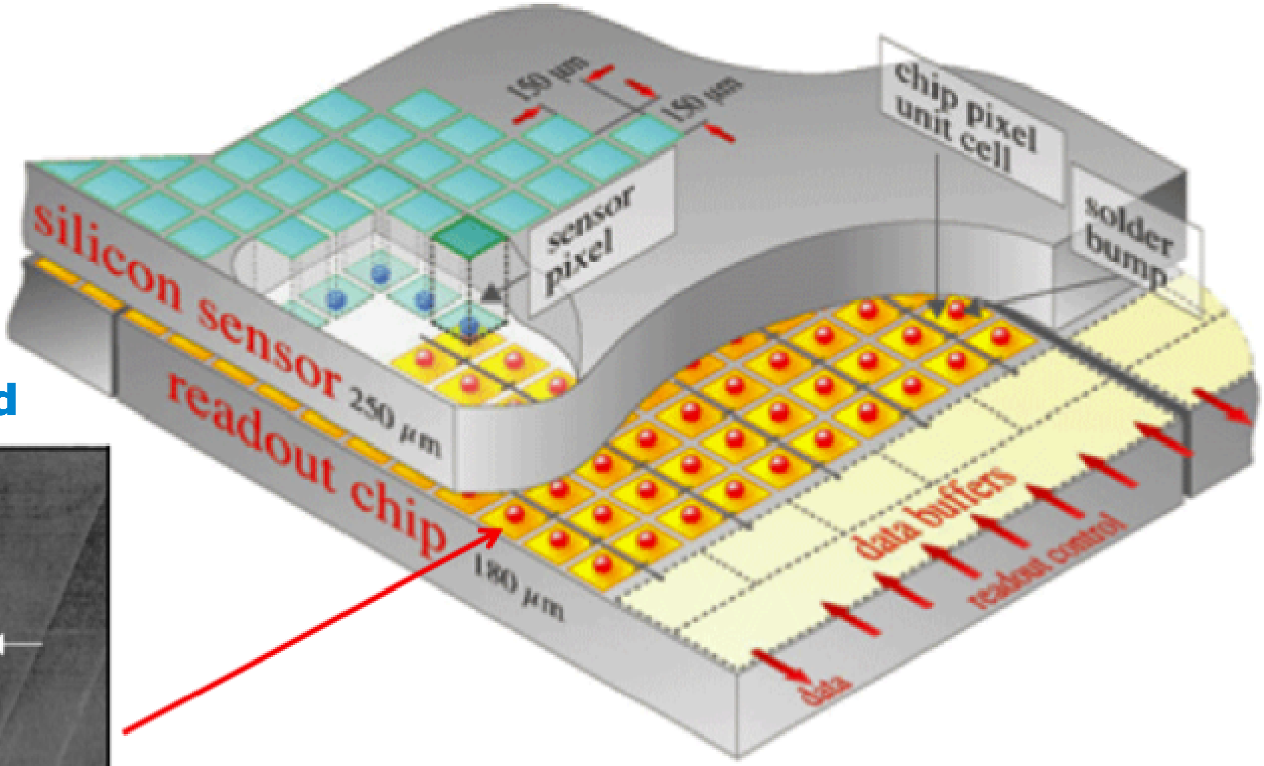

Hybrid Pixel Module for CMS

Sensor:

- Pixel Size: 150mm x 100mm
  - Resolution $\sigma_{r\text{-}\varphi}$ ~ 15µm
  - Resolution σ_z ~ 20µm
- n+-pixel on n-silicon design
  - Moderated p-spray → HV robustness

Readout Chip:

- Thinned to 175µm
- 250nm CMOS IBM Process
- 8” Wafer

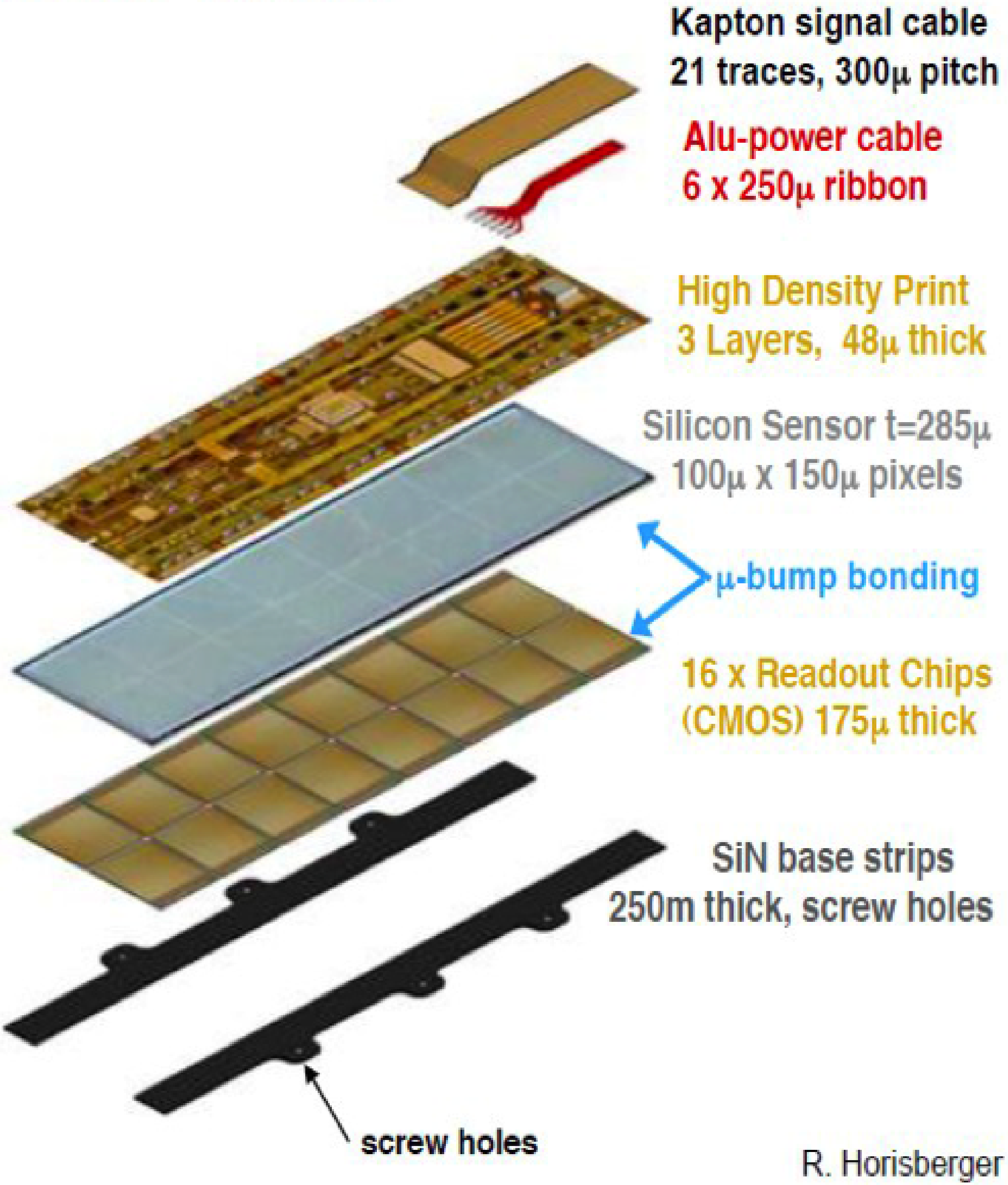

Performance: S/N

- **Signal** depends on the thickness of the depletion zone and on dE/dx of the particle

- **Noise** suffers contributions from:

$$\mathrm{ENC} = \sqrt{\mathrm{ENC}_C^2 + \mathrm{ENC}_I^2 + \mathrm{ENC}^2_{R_\parallel} + \mathrm{ENC}^2_{R_{series}}}$$

capacitance — leakage current — parallel resistor — series resistor

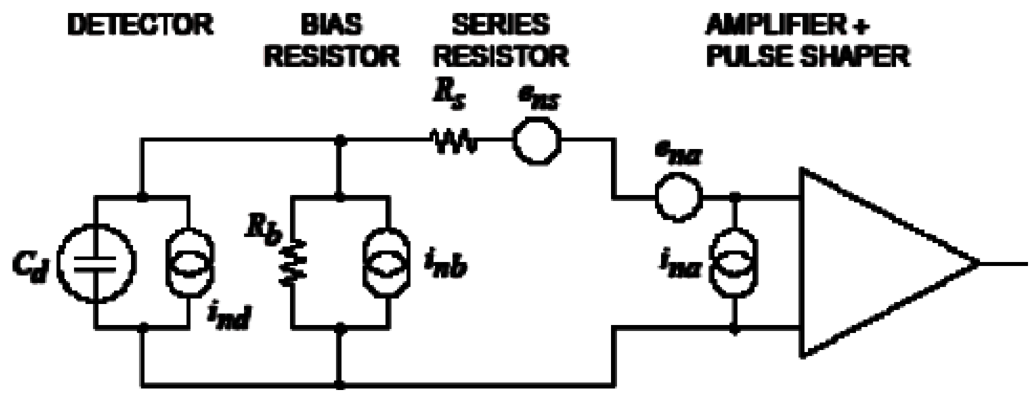

$$\mathrm{ENC}_{peak} = (36.6 \pm 1.9)\, e^- / \mathrm{cm} \cdot L + (405 \pm 27)\, e^-$$
$$\mathrm{ENC}_{dec} = (49.9 \pm 3.2)\, e^- / \mathrm{cm} \cdot L + (590 \pm 47)\, e^-$$

CMS strips

- **Optimizing S/N**
  - N_{ADC}>thr, given high granularity most channels are empty
  - decrease noise terms (see above)
  - minimize diffusion of charge cloud after thermal motion ▶ (typically ~8μm for 300μm drift)
  - radiation damage severely affects S/N (next slide)

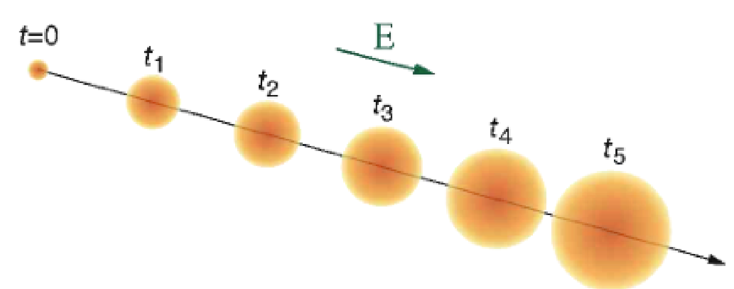

Influence of radiation

- In operation at the LHC **Si performance is affected by radiation -** e.g. from CMS
  - depletion voltage increases with fluence, kept within 500 V design limit
  - mild S/N degradation
  - expected hit finding efficiency after 10 years of LHC operation: 95%

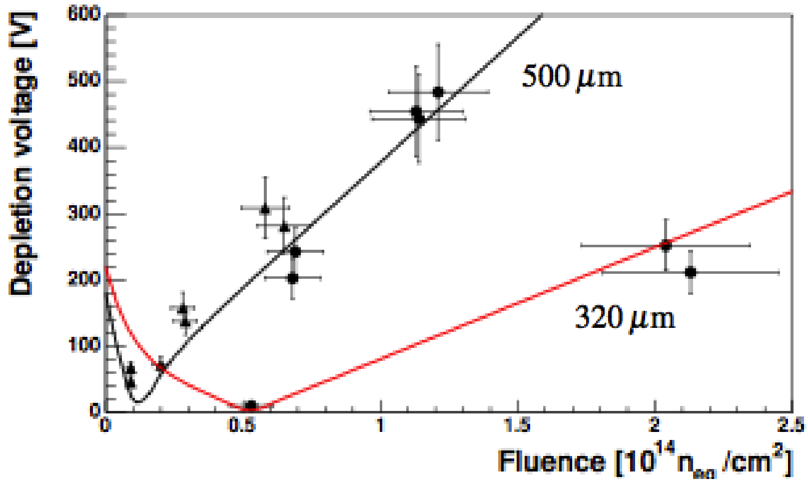

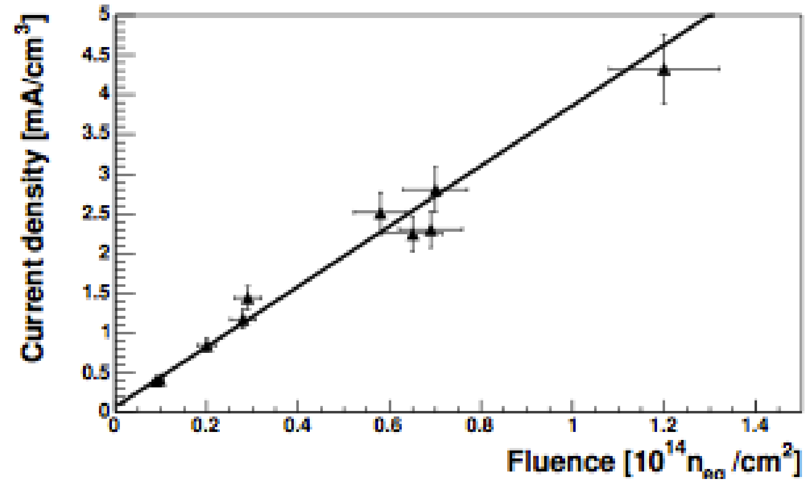

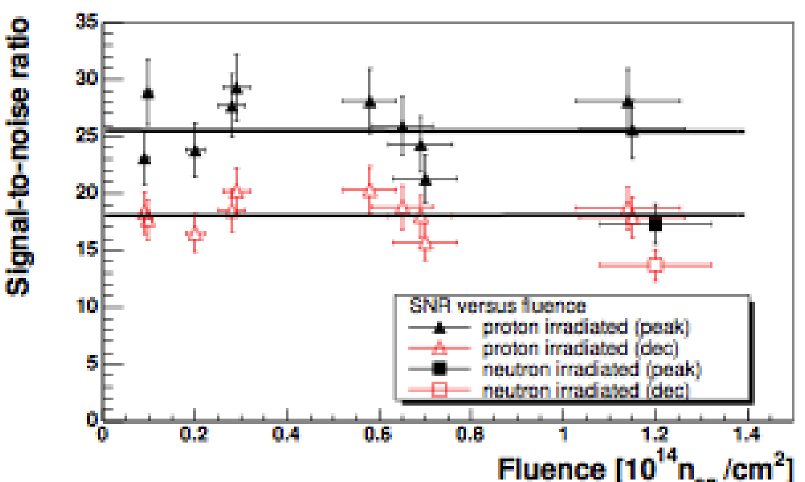

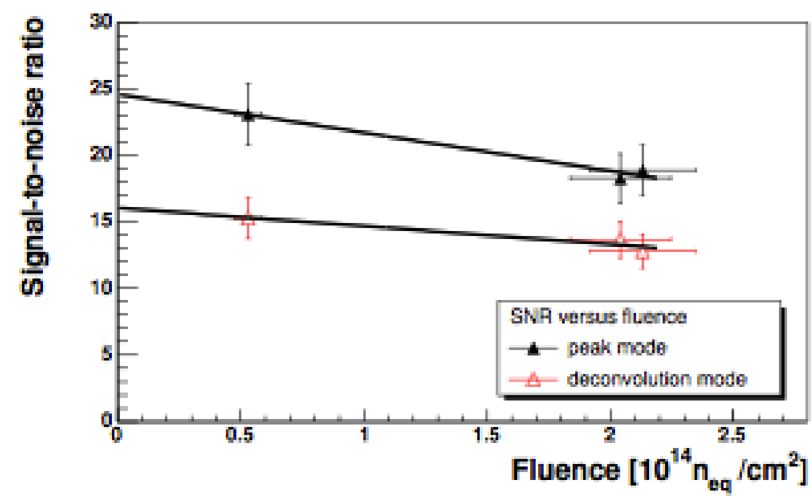

Position resolution

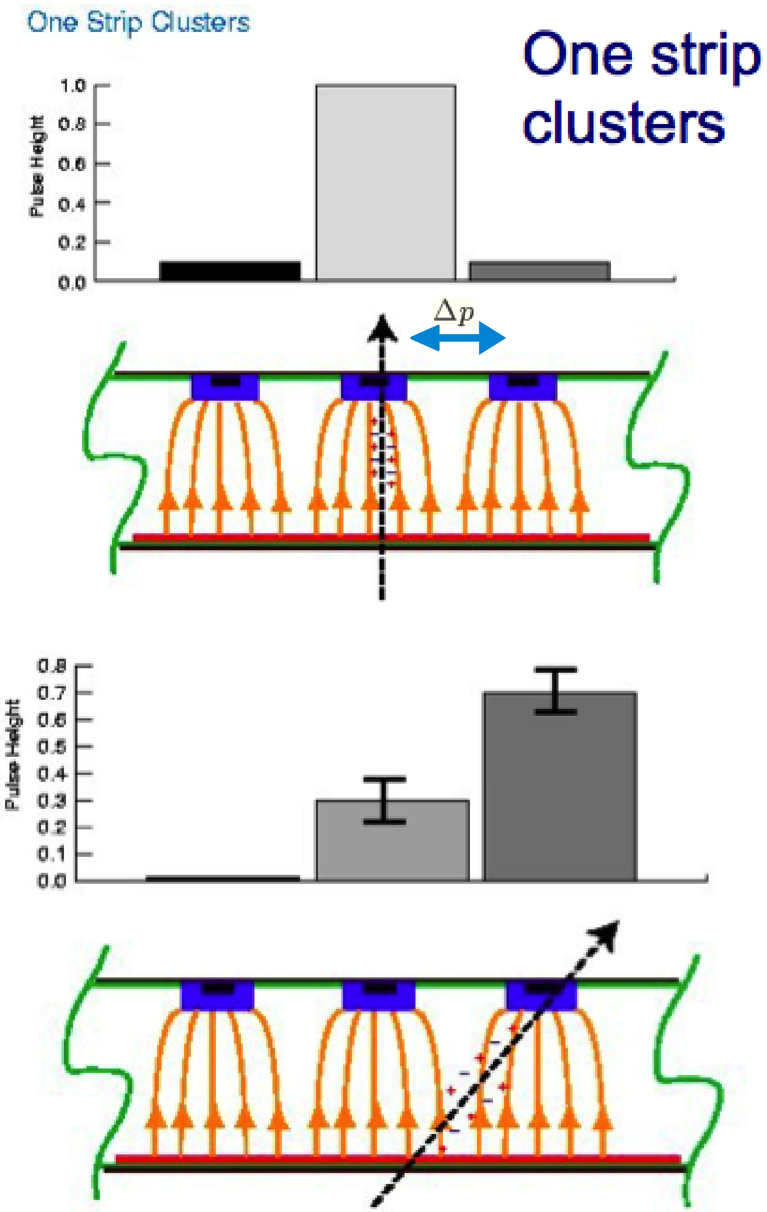

- Affected by different factors
  - transverse drift of electrons to track
  - strip pitch to diffusion width relationship
  - statistical fluctuations on energy deposition

$$\sigma_x \propto \frac{\Delta p}{S/N}$$

- Single strip resolution tends to dominate

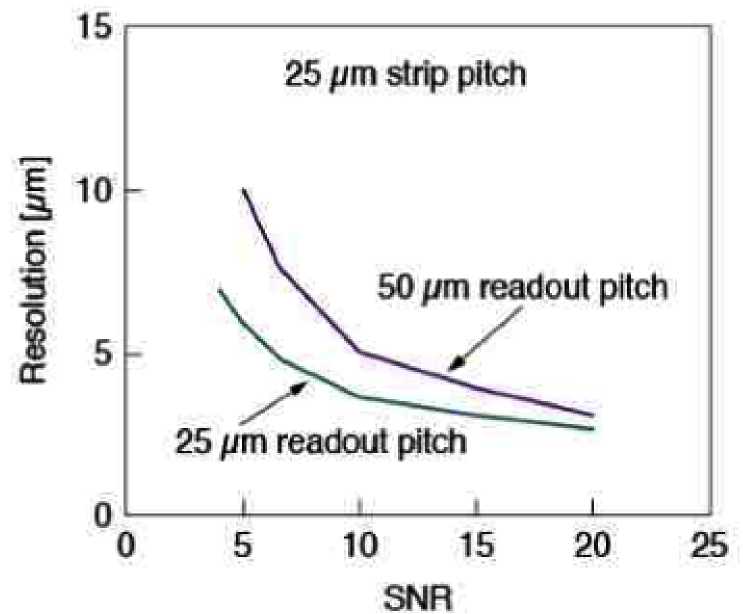

A. Peisert, *Silicon Microstrip Detectors*, DELPHI 92-143 MVX 2, CERN, 1992

Coordinates for tracking

- The LHC experiments use a uniform B field along the beam line (z-axis)
  - **Trajectory of charged particles is an helix** – radius R
  - Use transverse (xy) and longitudinal (rz) projections
  - Pseudo-rapidity: $\eta = -\ln \tan\frac{\theta}{2}$ Transverse momentum: $p_T = p \sin\theta = p / \cosh\eta$
- Impact parameter is defined from dca to origin or PV:

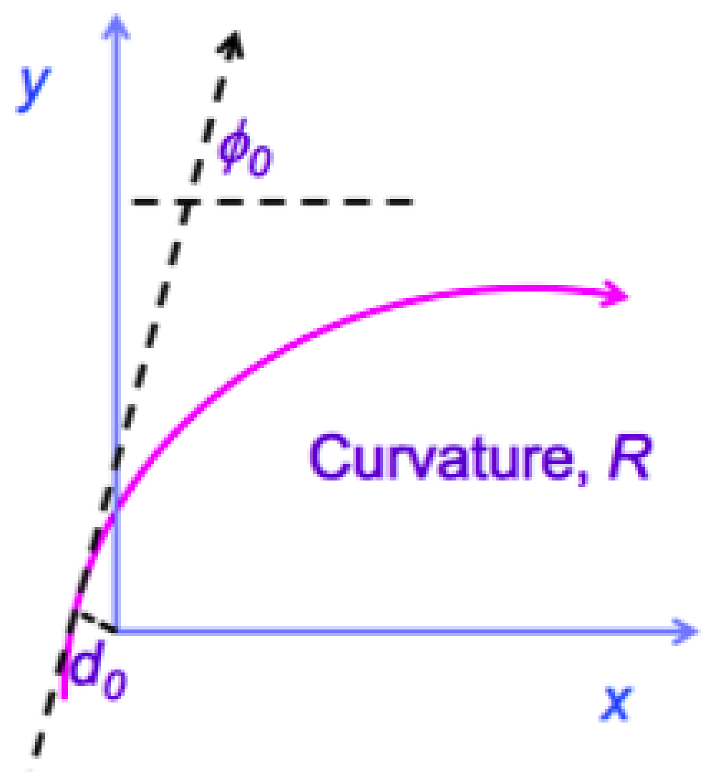

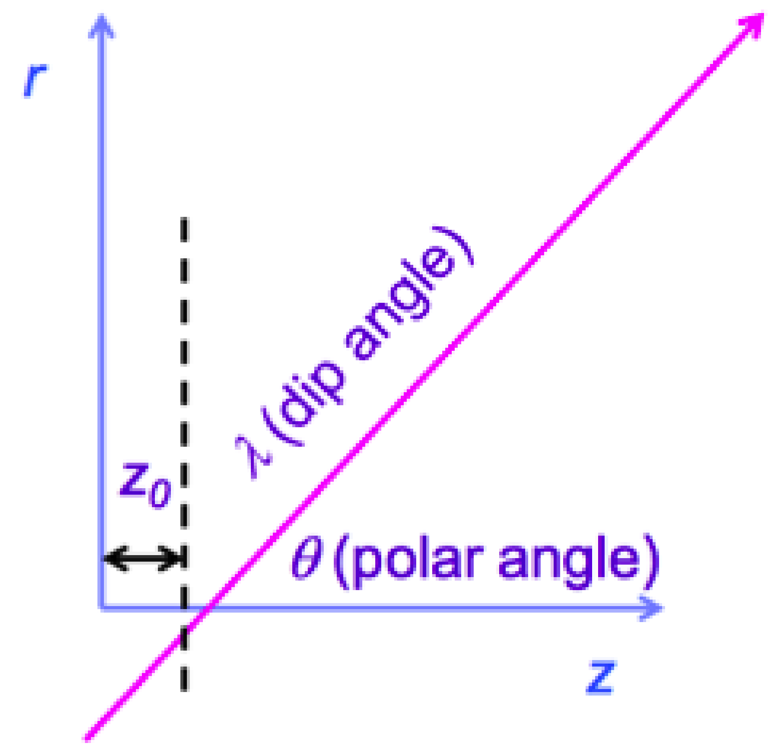

Resolution for the impact parameter

- **Depends on radii+space point precisions**

- For two layers we expect

$$\sigma_{d_0}^2 = \frac{r_2^2\sigma_1^2 + r_1^2\sigma_2^2}{(r_2 - r_1)^2}$$

  - Improve with small r_1, large r_2
  - Improves with better σ_i

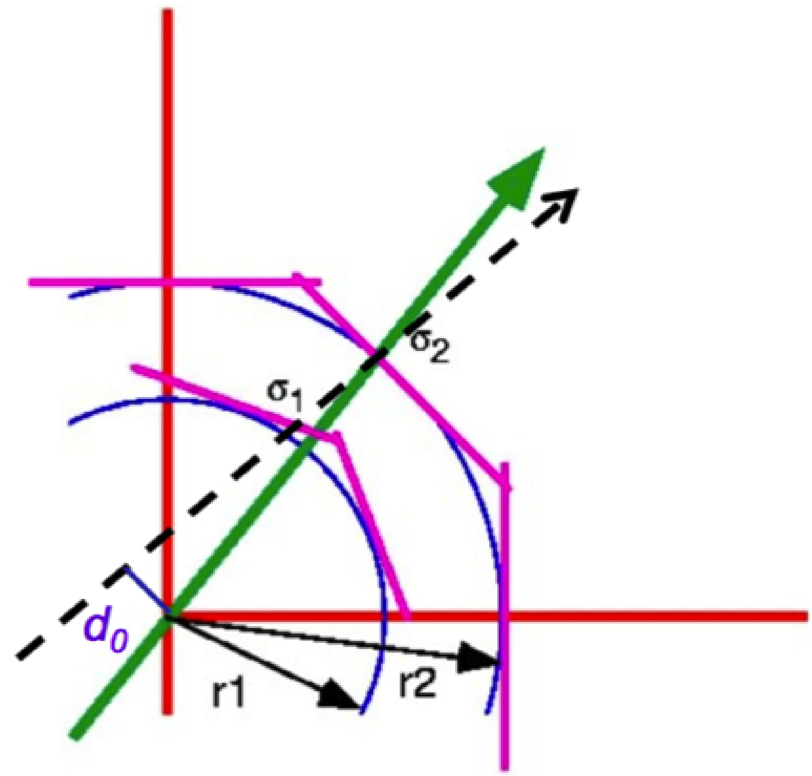

- Precision is degraded by **multiple scattering**
  - Gaussian approximation is valid with a rms width

$$\theta_0 = \frac{13.6\,\mathrm{MeV}}{\beta c p} z \sqrt{x/X_0}\left[1 + 0.038\ln(x/X_0)\right]$$

  - extra degradation term for d_0

$$\sigma_{d_0} \sim \theta_0$$

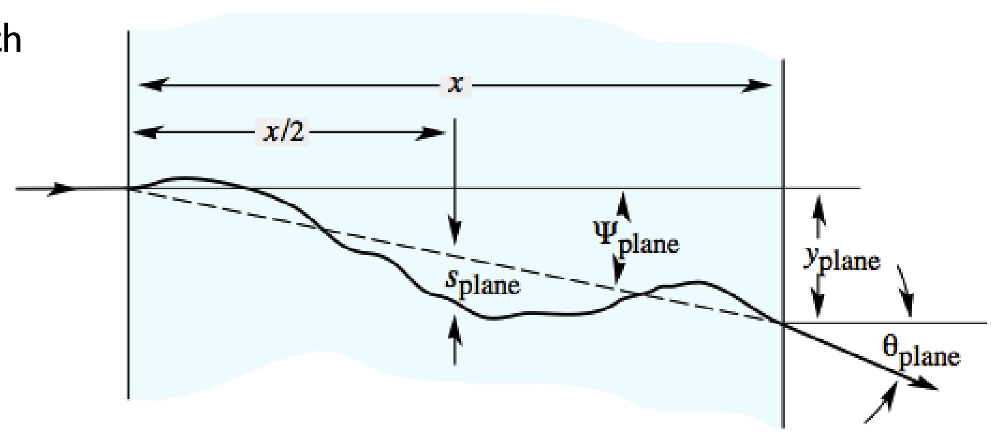

Resolution for the impact parameter

- For a track with θ≠90^0 we can write r → r/sinθ and x → x/sinθ
- By substitution in the formulas of the previous slide we have:

$$\sigma_{d_0} \sim \sqrt{\frac{r_2^2\sigma_1^2 + r_1^2\sigma_2^2}{(r_2 - r_1)^2}} \oplus \frac{r}{p\sin^{3/2}\theta} \rightarrow a \oplus \frac{b}{p_T \sin^{1/2}\theta}$$

geometry-dependent **Material- and p_T-dependent**

- **Resolution estimated with early pp data**
  - Observed

    100 µm @ 1 GeV

    20 µm @ 20 GeV
  - Excellent agreement with simulation

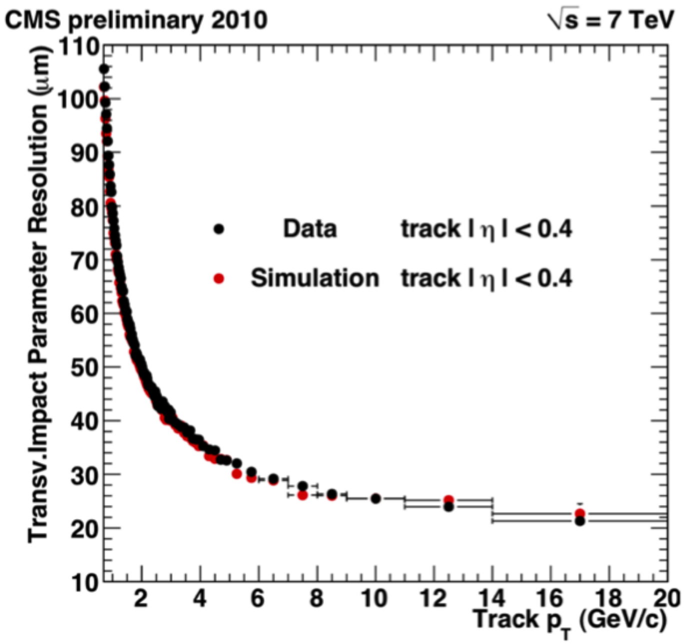

Examples from data: jets

- **Number of tracks** reconstructed in jets
  - two samples compared: multijets and top-pairs
  - track multiplicity is not well described by standard PYTHIA generator
  - $t \rightarrow Wb$ naturally enriches the top-pair sample in b-jets
  - B-hadrons are long-lived, b-jets often contain tracks with high d_0

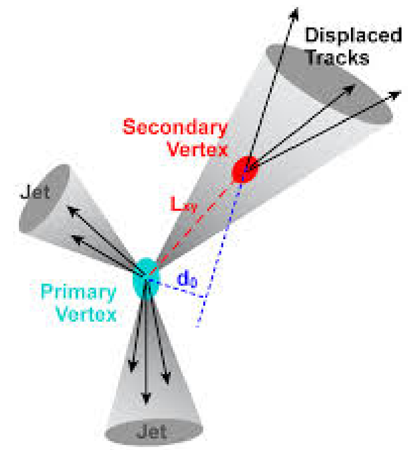

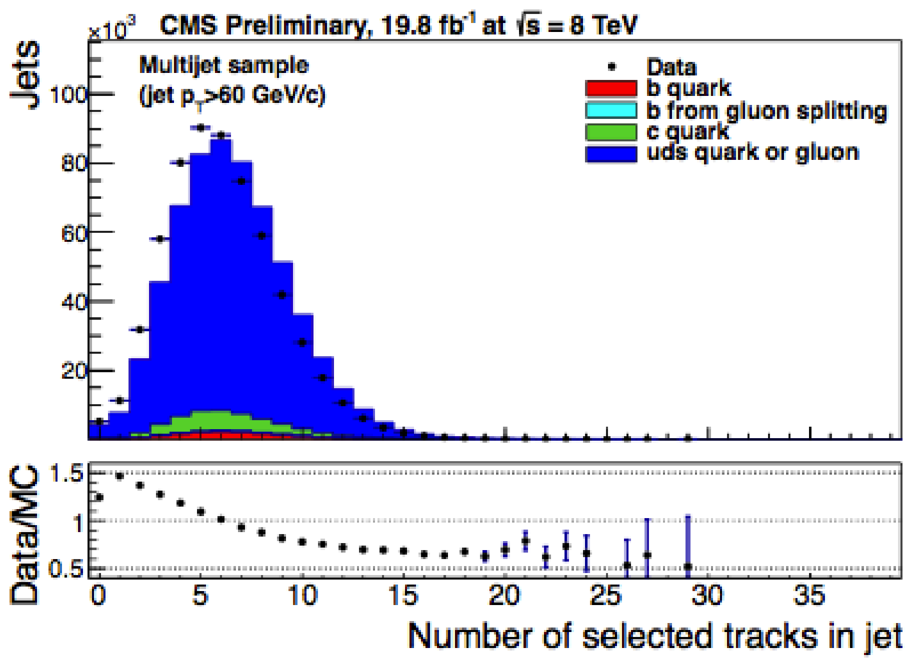

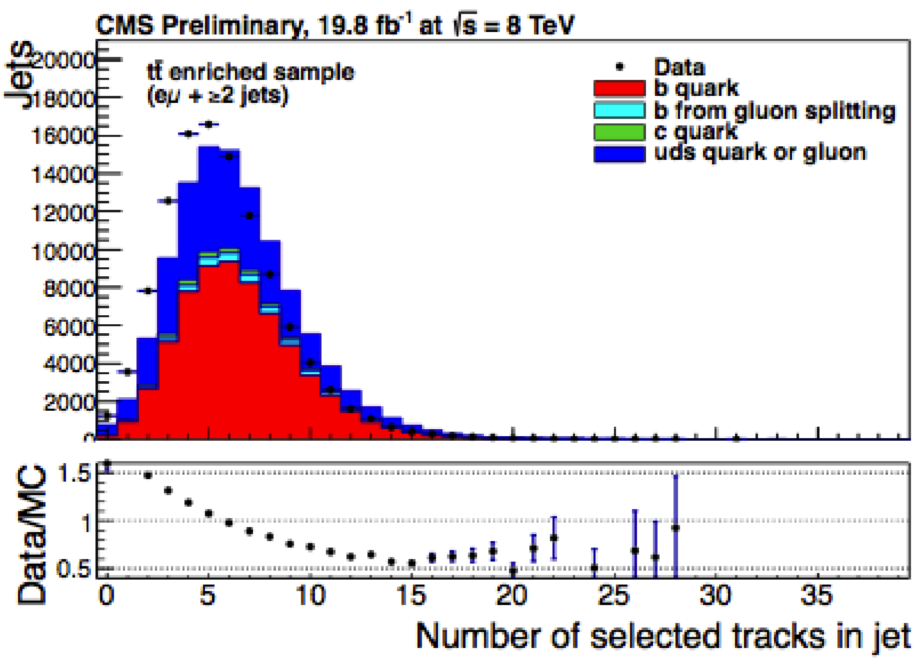

Examples from data: IP of tracks in jets

- Overall better agreement for b-jets: real displaced tracks
- Uncertainty on IP (resolution on IP) depends on the number of hits in pixels
    - ➔ jets from top pairs are more central with respect to a multijets sample

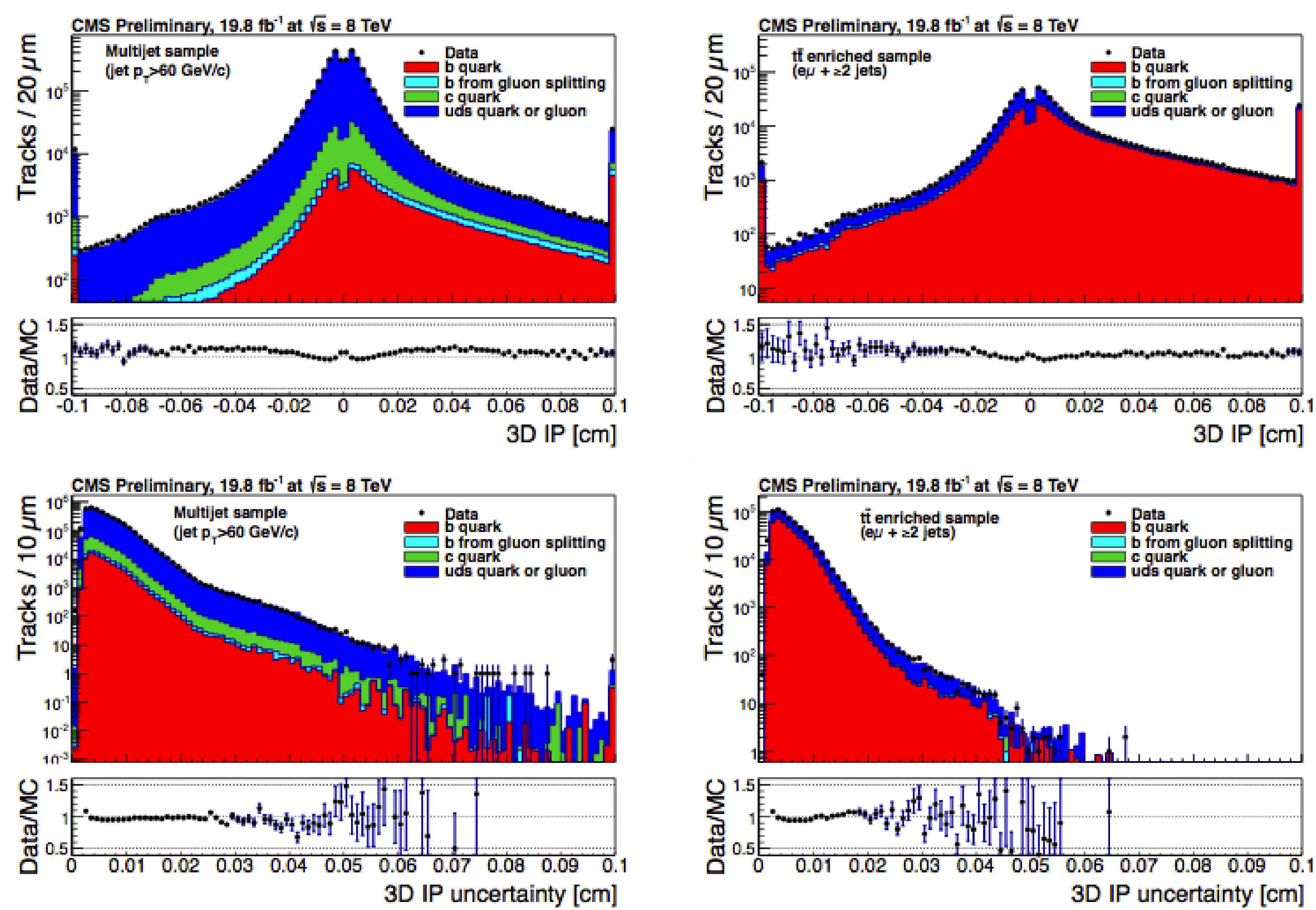

Examples from data: b-tagging from IP

- Distribution of the **third track with highest d_0/σ_{d0}**
  - Simple b-tagging algorithm, with high purity – track counting high purity (TCHP)
  - Good description of the b-jets
  - Light jets hard to model in simulation: multiple scattering, fake hits, missing hits, conversions, V_0 decays

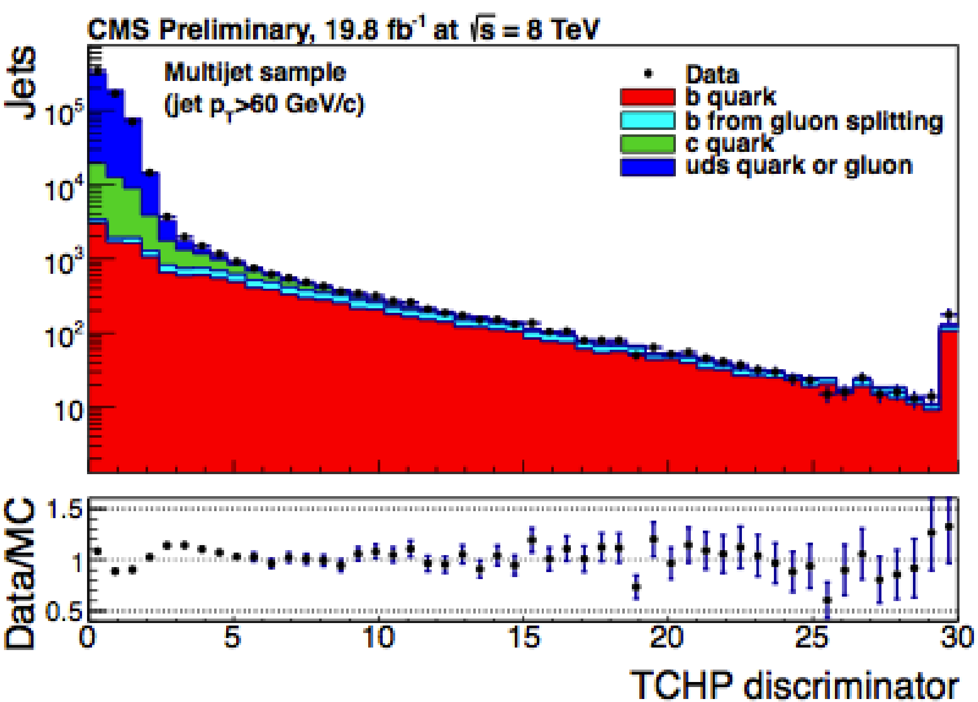

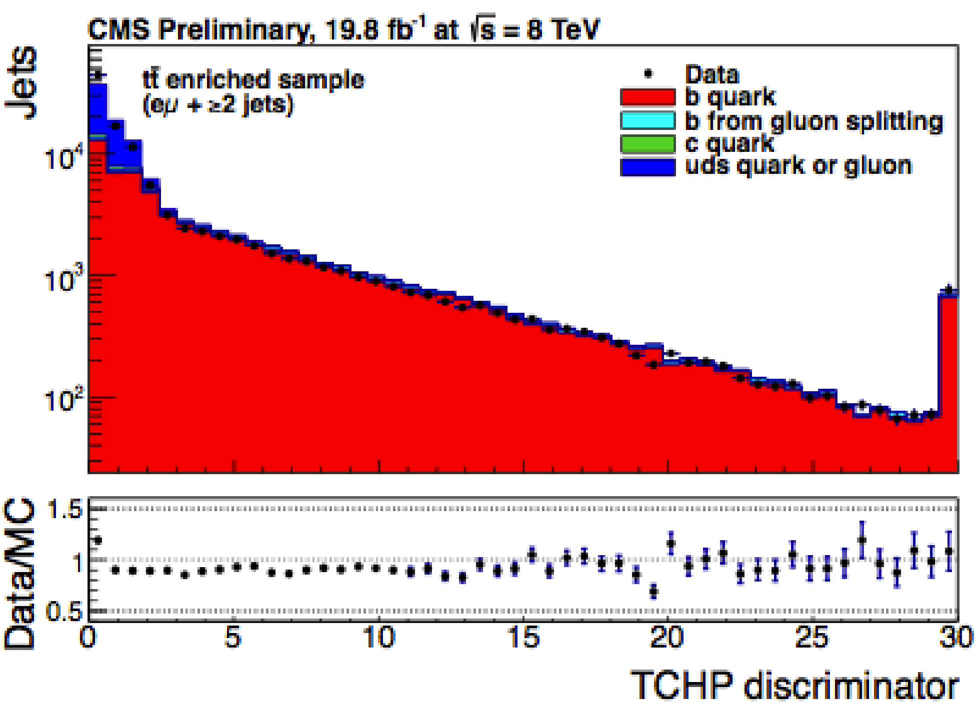

How can we profit from precision in d_0?

- ...it's not only the b-tagging performance that benefits
- Can use measurement of the displaced vertices to measure fundamental properties
- **Boost of B-hadrons: proportional to the mass of a top quark when t→ Wb**
  - $L_{xy} = \gamma_B \beta_B \tau_B \approx 0.4 \frac{m_t}{m_B} \beta_B \tau_B$
  - Average shift of 30μm per 1 GeV
  - Use observed media to measure m_t

$$m_t = 173.5 \pm 1.5_{stat} \pm 1.3_{syst} \pm 2.6_{p_T(top)} \mathrm{GeV}$$

  - Simple, robust observables can measure fundamental properties

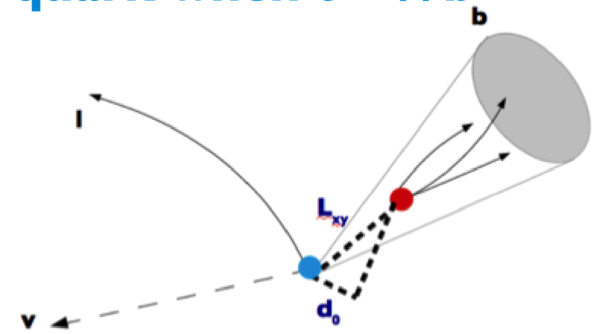

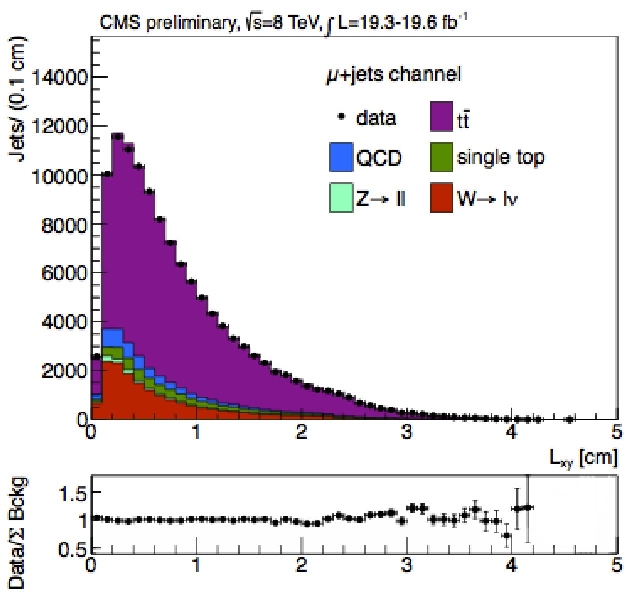

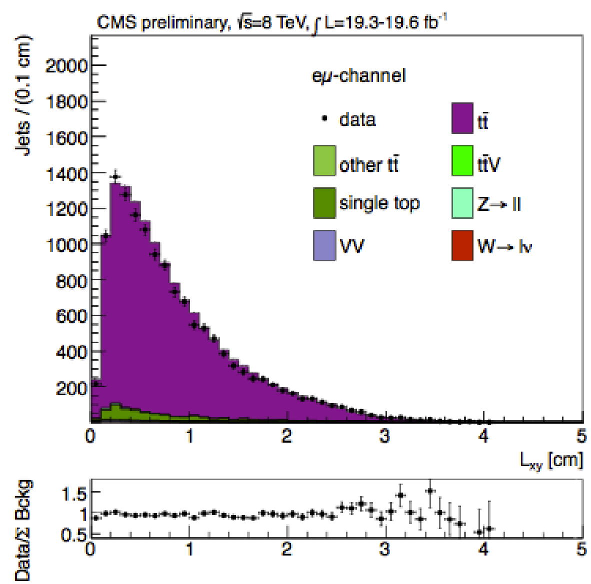

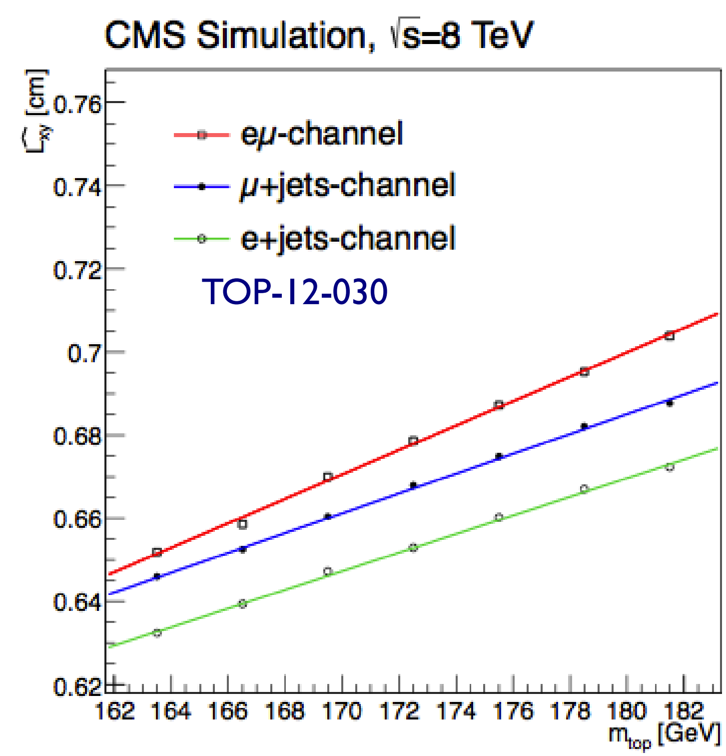

Momentum measurement

- Circular motion under uniform B-field

$$R[m] = 0.3\frac{B[T]}{p_T[GeV]}$$

- **Measure sagitta**, s, from track ark
  - yields R estimate:

$$R = \frac{L^2}{2s} + \frac{s}{2} \approx \frac{L^2}{2s}$$

  - relate to B and estimate p_T

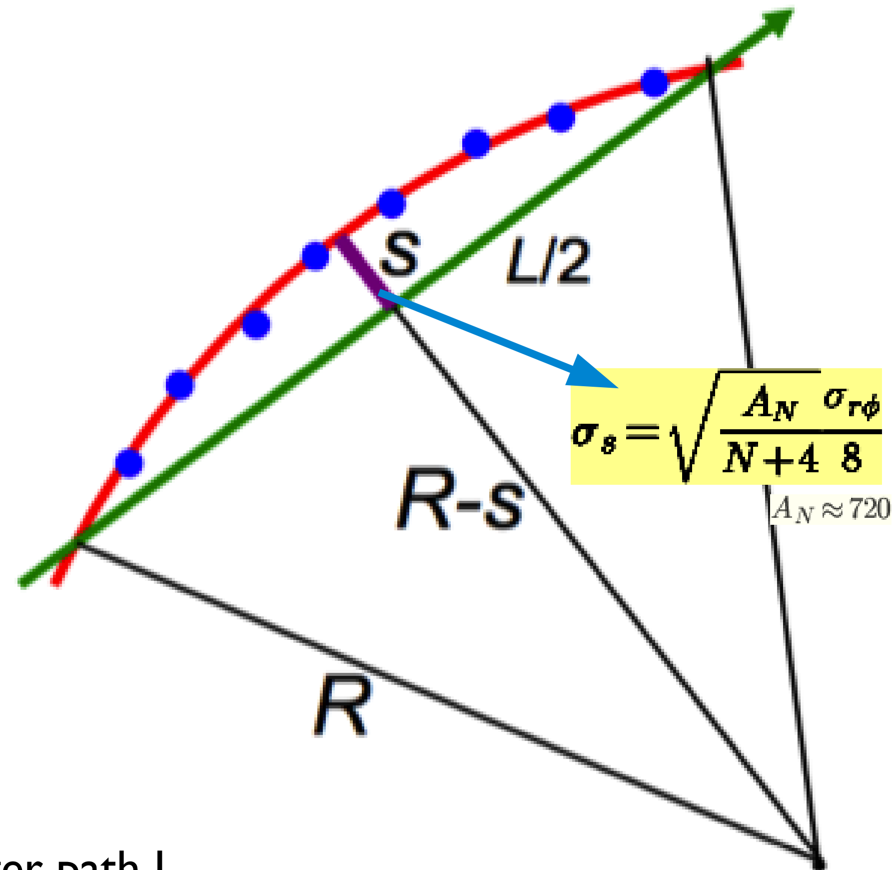

- Uncertainty improves with B, number of hits, longer path L

$$\frac{\sigma_{p_T}}{p_T} = \frac{8p_T}{0.3BL^2}\sigma_s$$

- **Again, spoiled with multiple scattering:**

$$\frac{\sigma_{p_T}}{p_T} \sim a p_T \oplus \frac{b}{\sin^{1/2}\theta}$$

Momentum resolution

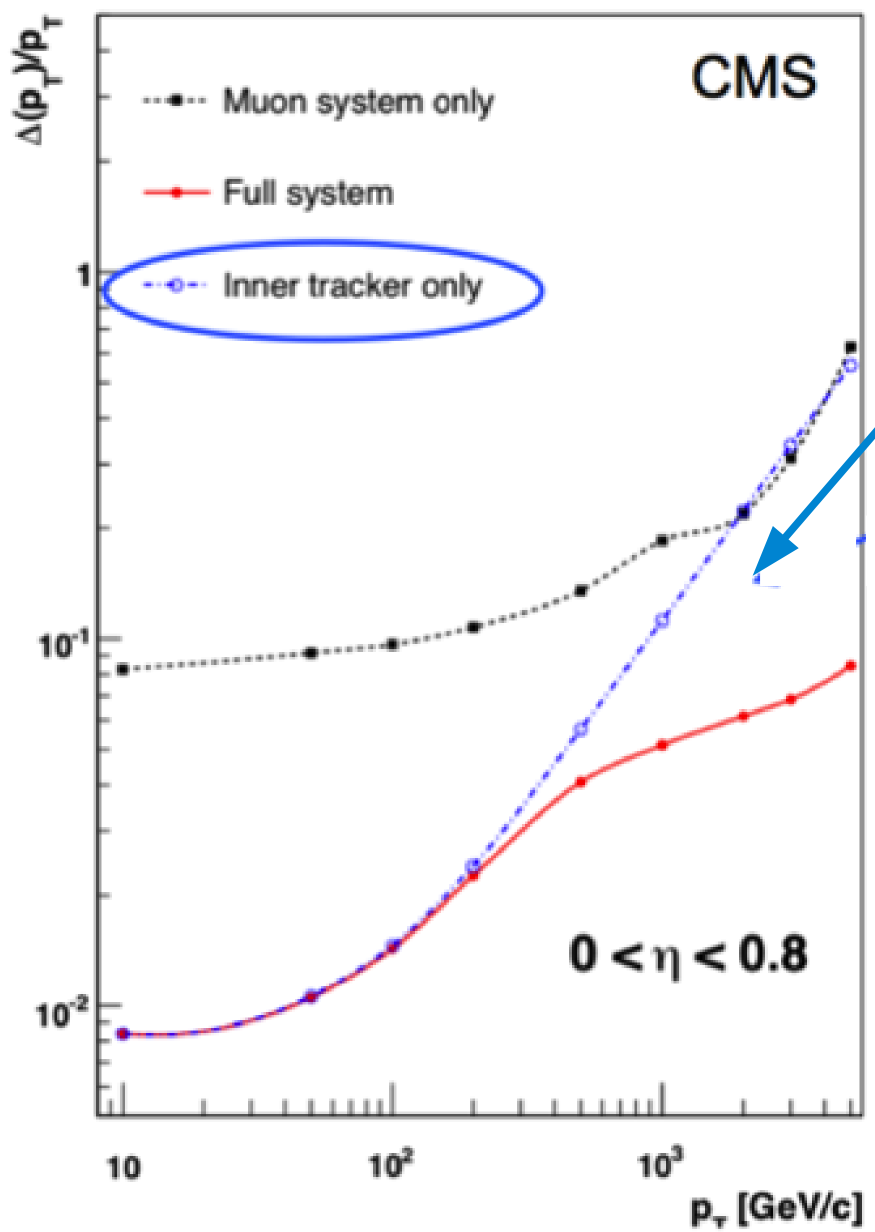

$$\frac{\sigma_{p_T}}{p_T} \sim a\, p_T \oplus \frac{b}{\sin^{1/2}\theta}$$

$$\theta = 2\arctan(e^{-\eta})$$

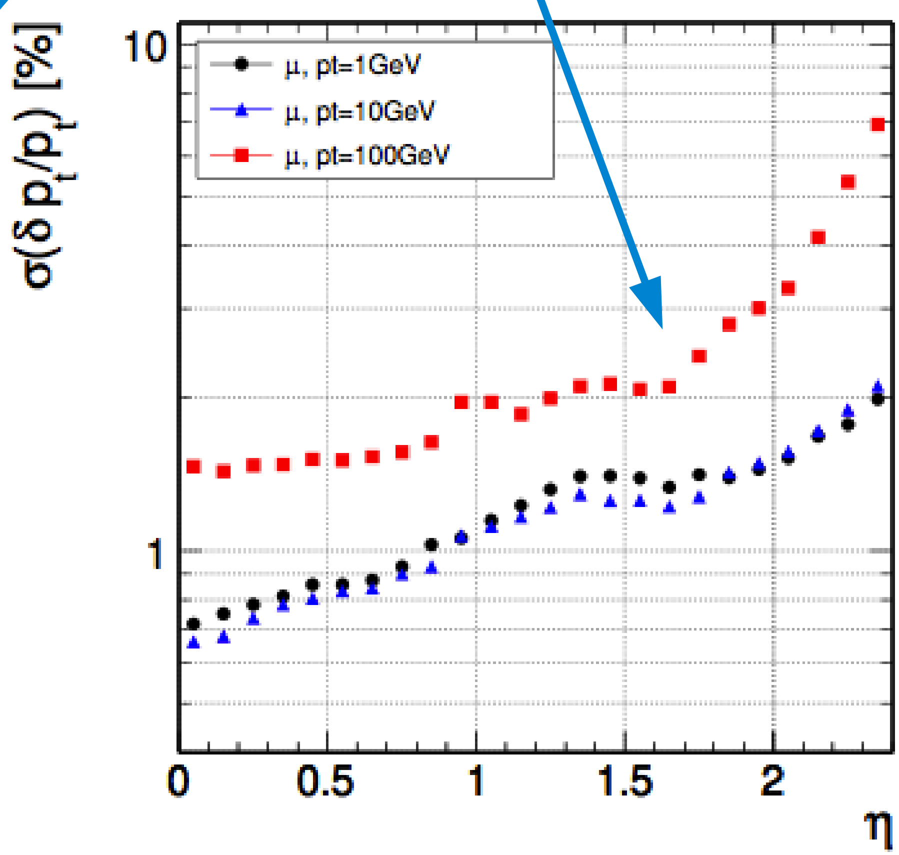

Performance: ATLAS vs CMS

	ATLAS	CMS
Reconstruction efficiency for muons with $p_T = 1$ GeV	96.8%	97.0%
Reconstruction efficiency for pions with $p_T = 1$ GeV	84.0%	80.0%
Reconstruction efficiency for electrons with $p_T = 5$ GeV	90.0%	85.0%
Momentum resolution at $p_T = 1$ GeV and $\eta \approx 0$	1.3%	0.7%
Momentum resolution at $p_T = 1$ GeV and $\eta \approx 2.5$	2.0%	2.0%
Momentum resolution at $p_T = 100$ GeV and $\eta \approx 0$	3.8%	1.5%
Momentum resolution at $p_T = 100$ GeV and $\eta \approx 2.5$	11%	7%
Transverse i.p. resolution at $p_T = 1$ GeV and $\eta \approx 0$ (μm)	75	90
Transverse i.p. resolution at $p_T = 1$ GeV and $\eta \approx 2.5$ (μm)	200	220
Transverse i.p. resolution at $p_T = 1000$ GeV and $\eta \approx 0$ (μm)	11	9
Transverse i.p. resolution at $p_T = 1000$ GeV and $\eta \approx 2.5$ (μm)	11	11
Longitudinal i.p. resolution at $p_T = 1$ GeV and $\eta \approx 0$ (μm)	150	125
Longitudinal i.p. resolution at $p_T = 1$ GeV and $\eta \approx 2.5$ (μm)	900	1060

- CMS tracker outperforms ATLAS: better momentum resolution, similar vertexing
- However it comes with a cost (next slide)

CMS tracker

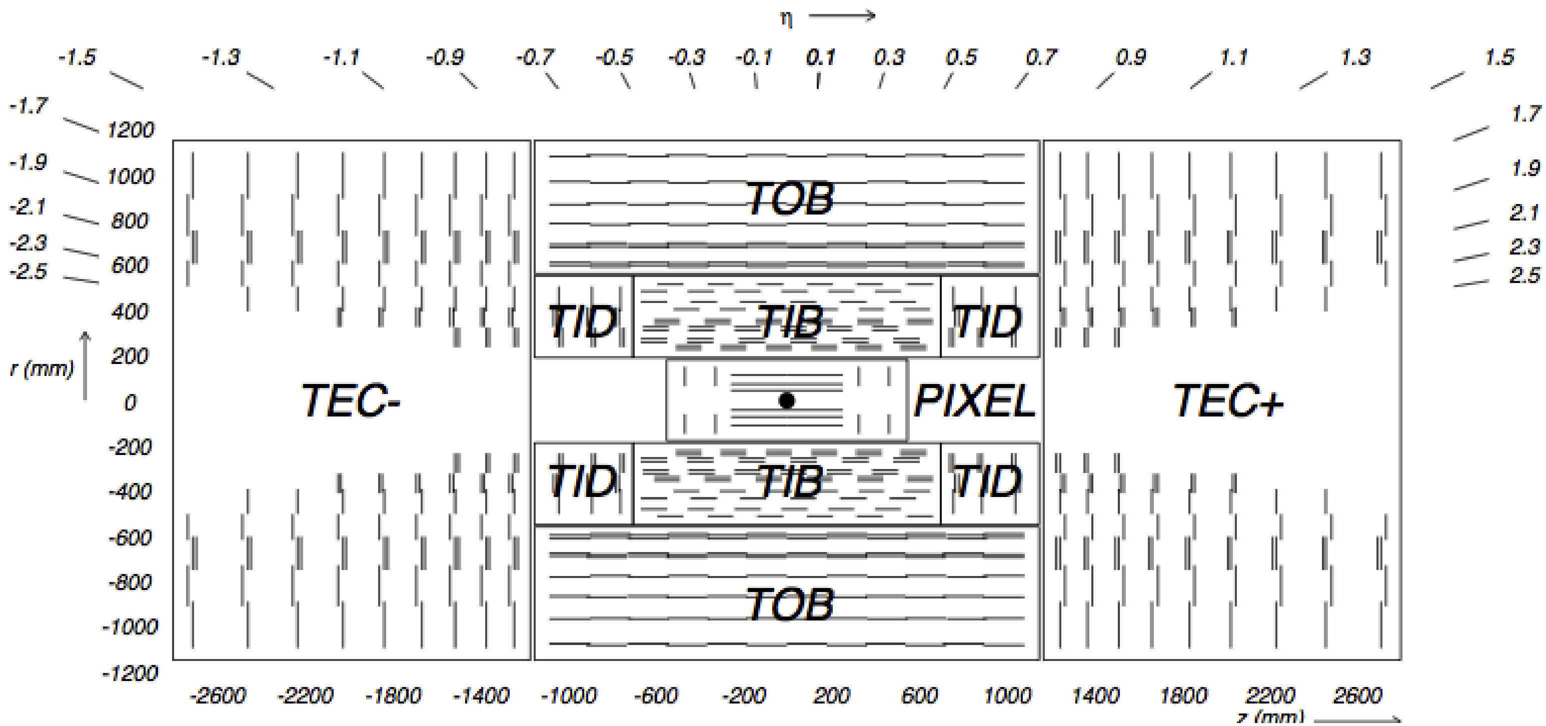

- Pixel detector: ~1m² area
  - 1.4k modules
  - 66M pixels
- Strips: ~200m² area
  - 24k single sensors, 15k modules
  - 9.6M strips = electronics channels
  - 75k readout chips

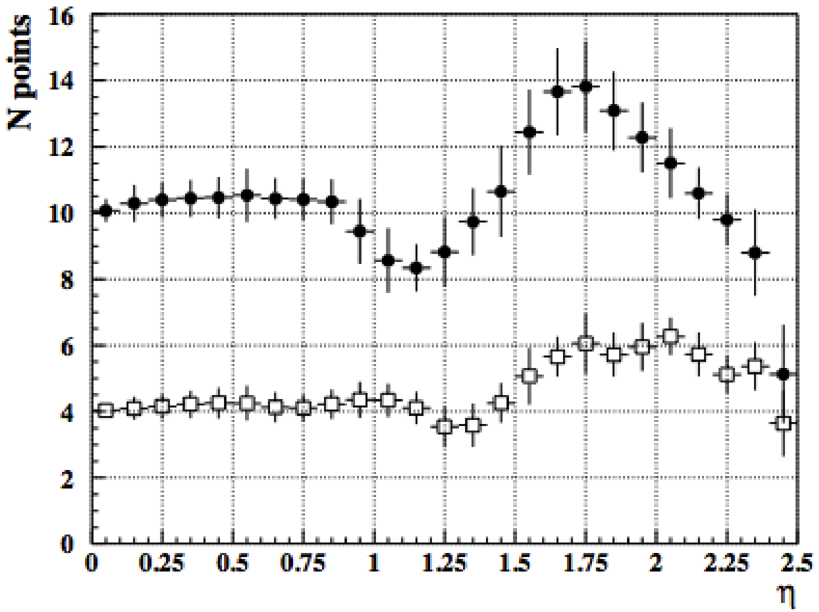

CMS tracker budget

- In some regions can attain $1.8X_0 \rightarrow$ photons convert, electrons radiate often
- Use for alignment and material budget estimation
  - Simulation crucial for $H \rightarrow \gamma\gamma$, $H \rightarrow ZZ \rightarrow 2e2\mu, 4e$

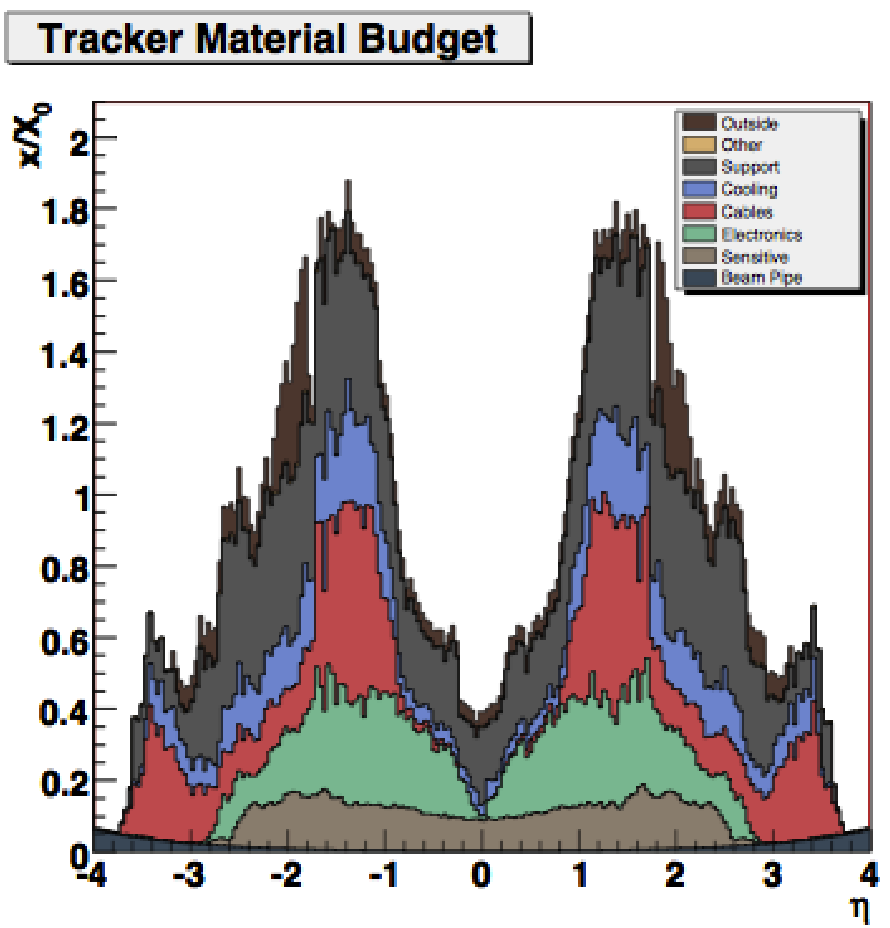

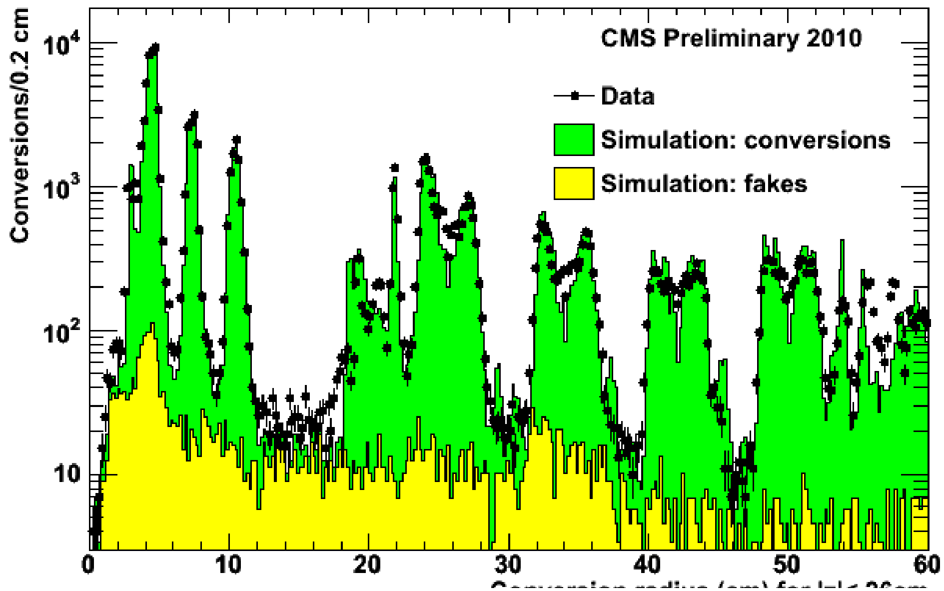

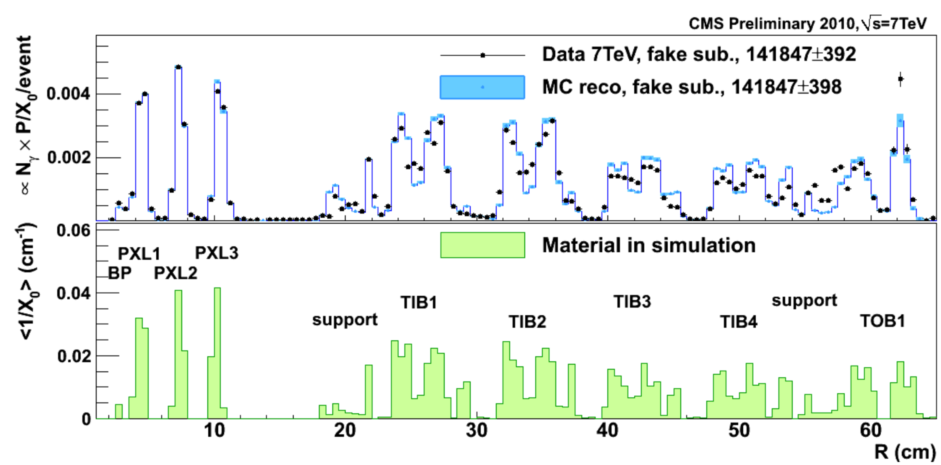

X-ray of the CMS tracker

- Conversions: $\gamma \rightarrow e^+e^-$
  - two op. Charged tracks consistent from the same point
  - consistent with fit to a common vertex with M=0 GeV
  - Note: 54% of the $H \rightarrow \gamma\gamma$ events have are expected to have at least one conversion

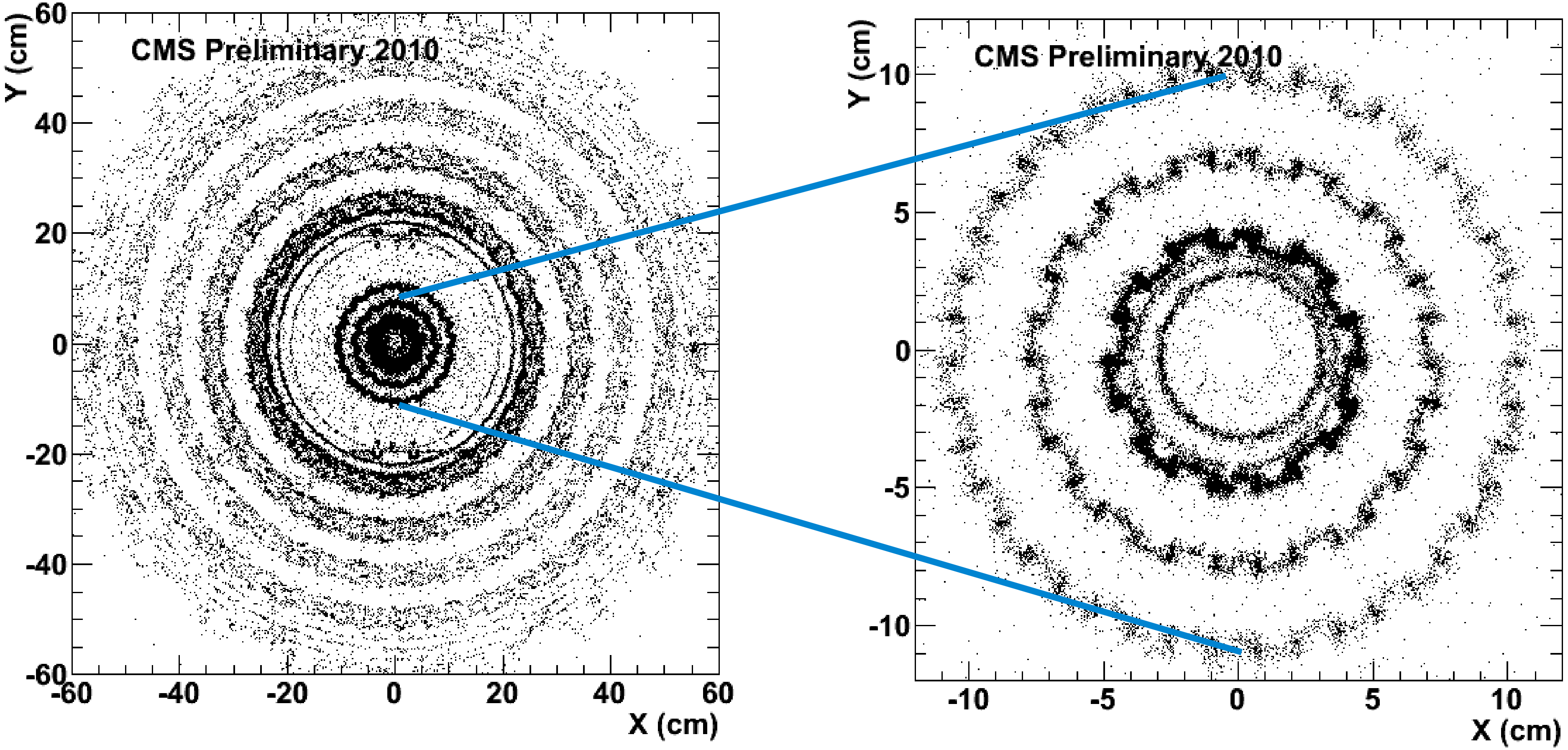

Alignment check

- Use reconstructed long-lived neutral hadrons to compare simulation, PDG and data

V^0	Mass (MeV/c^2)			
	Data	PDG	Simulation	Generated
K^0_S	497.68 ± 0.06	497.61 ± 0.02	498.11 ± 0.01	497.670
Λ^0	1115.97 ± 0.06	1115.683 ± 0.006	1115.93 ± 0.02	1115.680

Parameter	K^0_S Data	K^0_S Simulation	Λ^0 Data	Λ^0 Simulation
$\sigma_1 (\mathrm{MeV}/c^2)$	4.53 ± 0.12	4.47 ± 0.04	1.00 ± 0.26	1.71 ± 0.05
$\sigma_2 (\mathrm{MeV}/c^2)$	11.09 ± 0.41	10.49 ± 0.11	3.25 ± 0.14	3.71 ± 0.09
σ_1 fraction	0.58 ± 0.03	0.58 ± 0.01	0.15 ± 0.05	0.44 ± 0.03
$\bar{\sigma} (\mathrm{MeV}/c^2)$	7.99 ± 0.14	7.63 ± 0.03	3.01 ± 0.08	2.99 ± 0.03

$\tau_{K^0_S} = 90.0 \pm 2.1\,\mathrm{ps}$ $\tau_{\Lambda^0} = 271 \pm 20\,\mathrm{ps}$ *, both consistent with world average*

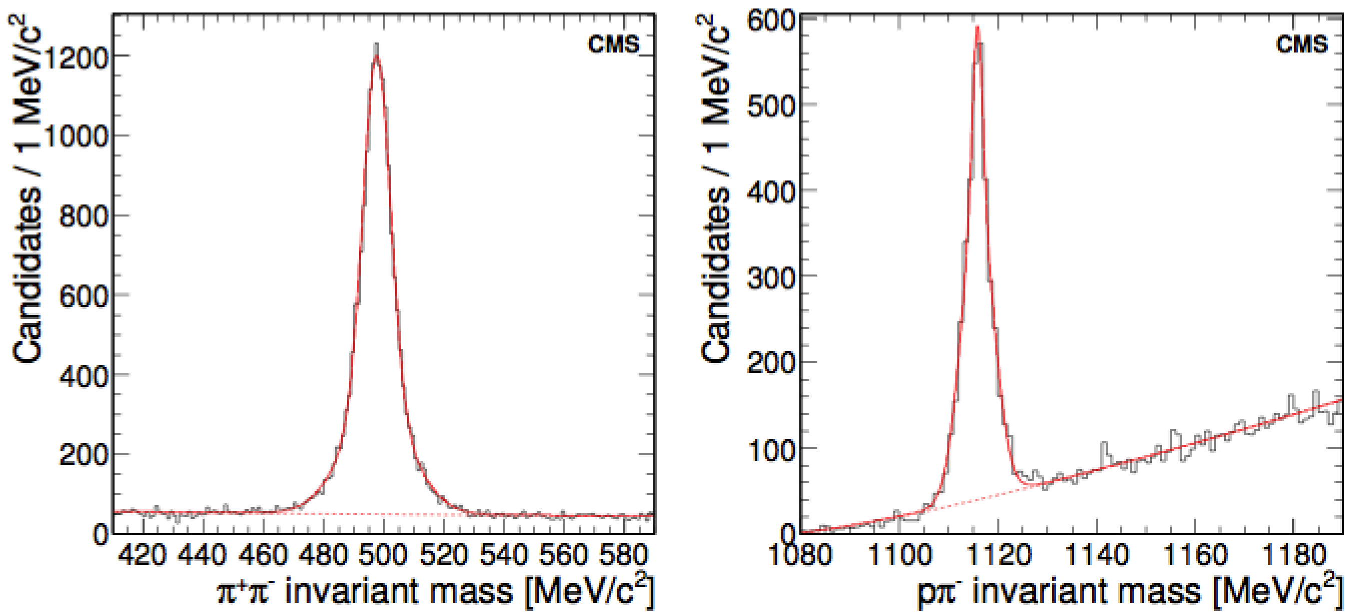

Outer tracking

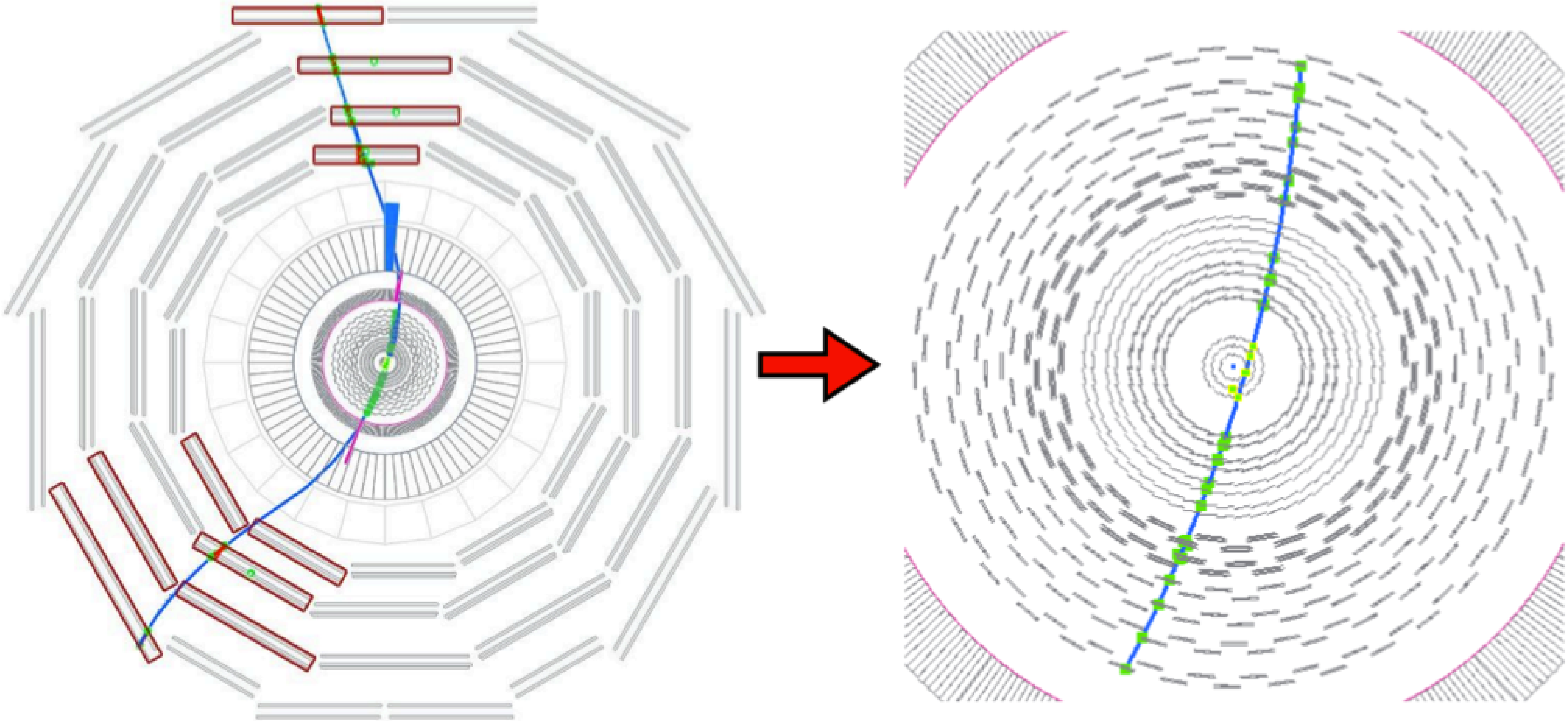

Find muons with the tracking system

- Standard-approach: **outside-in**
  - Standalone muon
  - Combine with tracker track
  - Fit a Global Muon track
- Complementary approach: **inside-out**
  - Extrapolate every track outward
  - Find compatible deposits in calorimeters
  - Define muon compatibility
- **Recovers inefficiencies**
  - Boundaries of muon chambers, low p_T

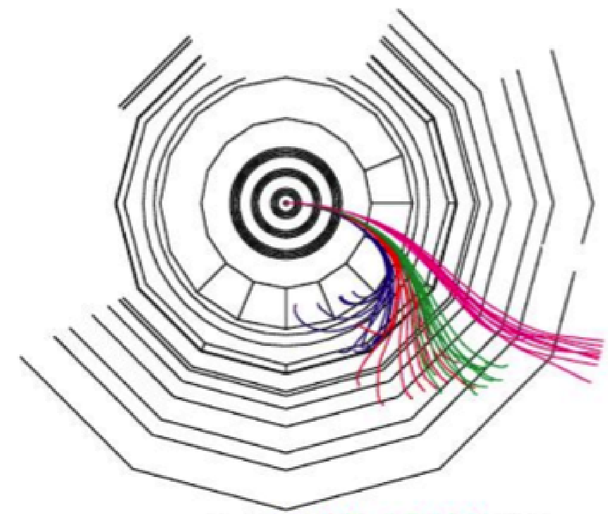

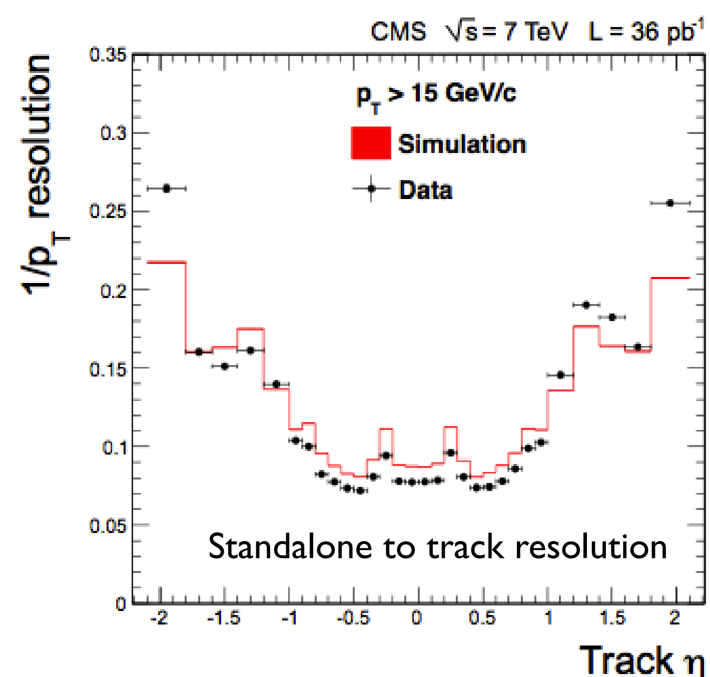

Performance: ATLAS vs CMS II

ATLAS

- B=0.7 T (toroidal)
- L~5m
- N=3 stations x 8 points

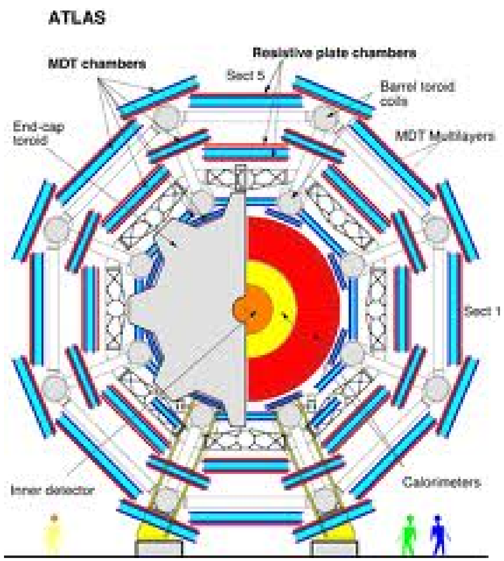

- s=750 μm for 1 TeV track
- 10% → σ=75 μm

Δp/p~6%

CMS

- B~2T (in return yoke)
- L~3.5m
- N=4 stations x 8 points in rφ

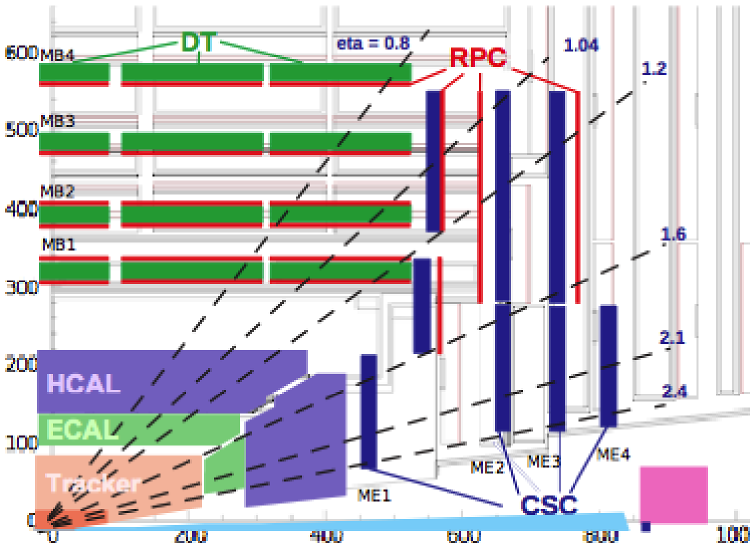

- s=900 μm for 1 TeV track
- 10% → s=90μm

Δp/p~12%

Spoiled by multiple scattering in Fe

Combined muon performance in CMS

Combine with tracker: Δp/p~2%

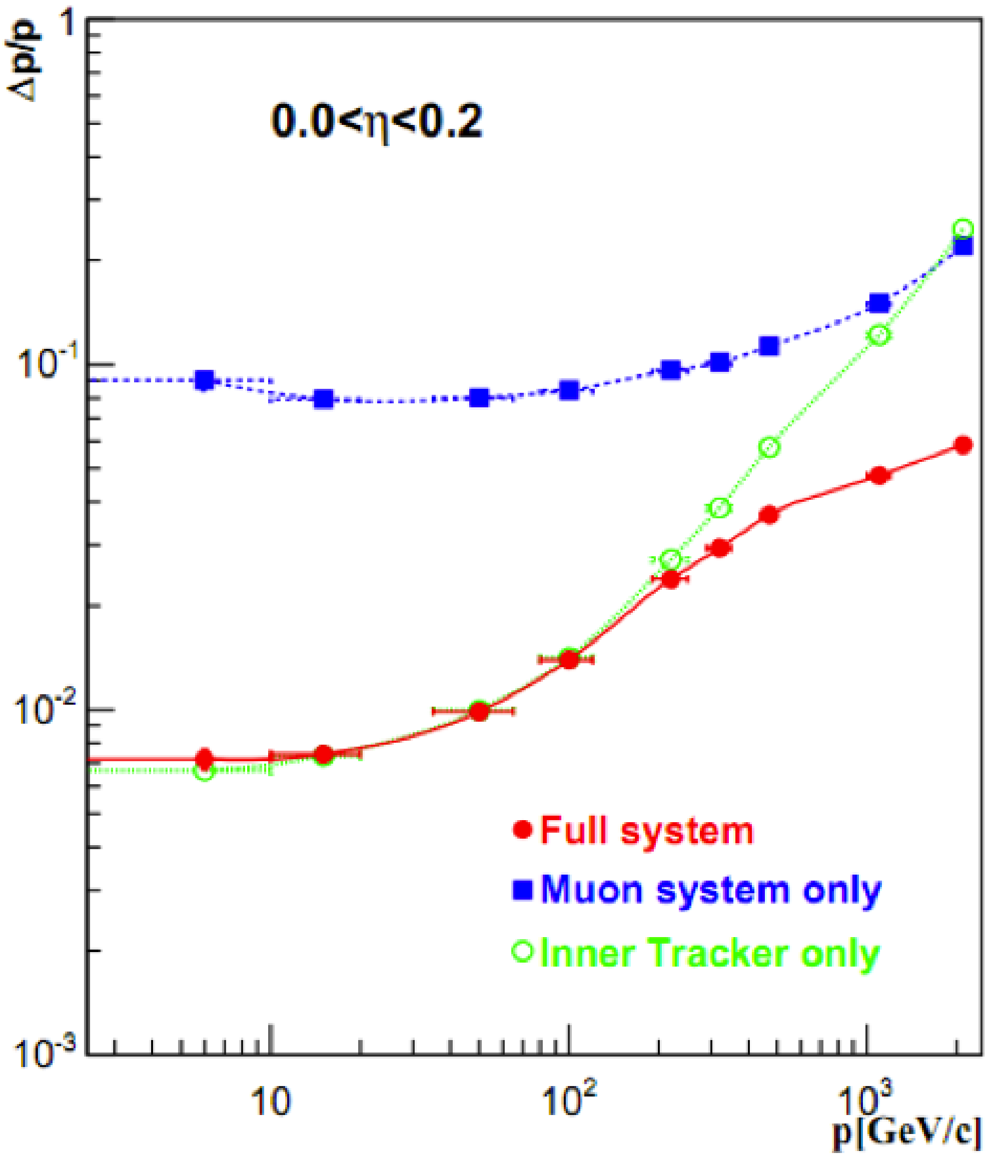

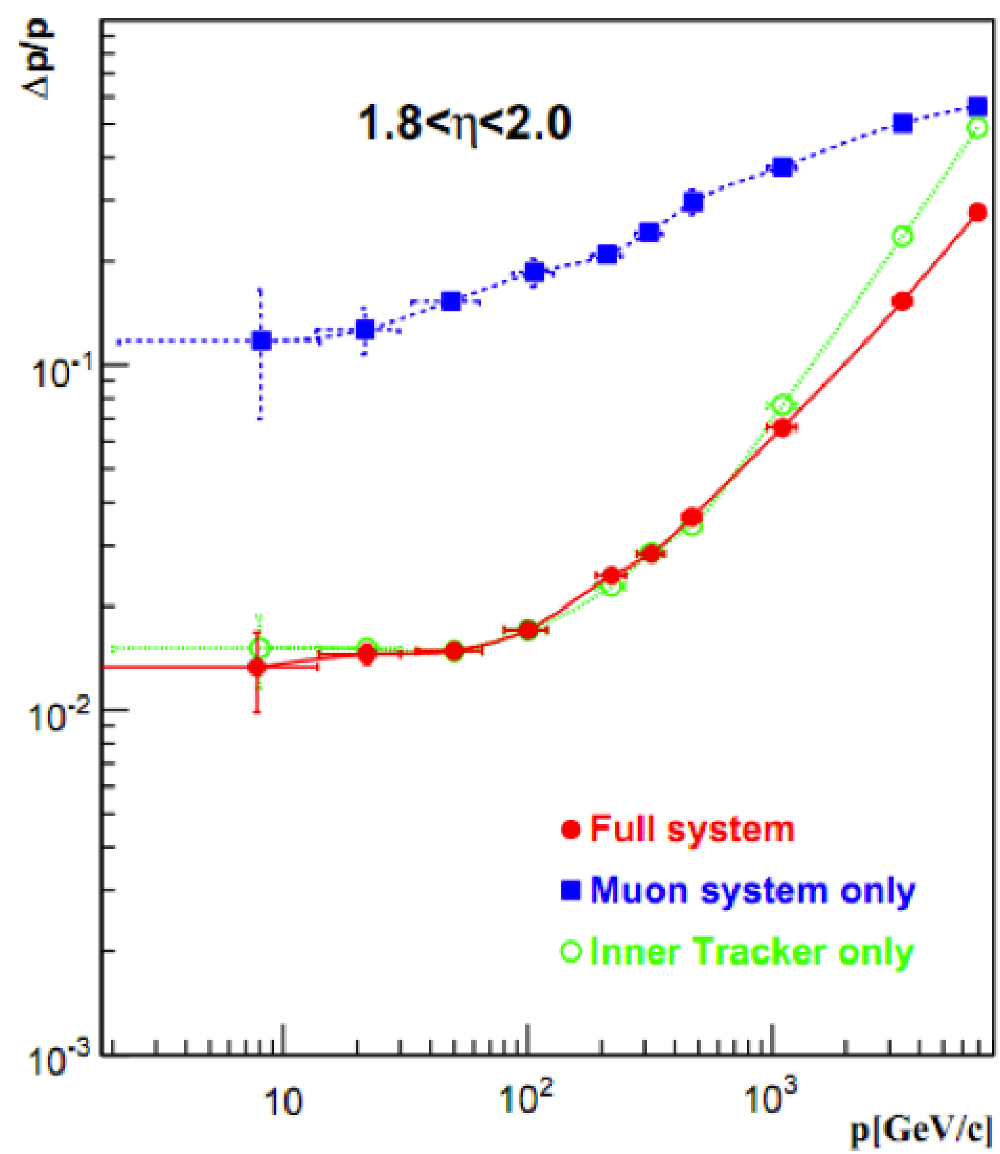

CMS dimuon performance

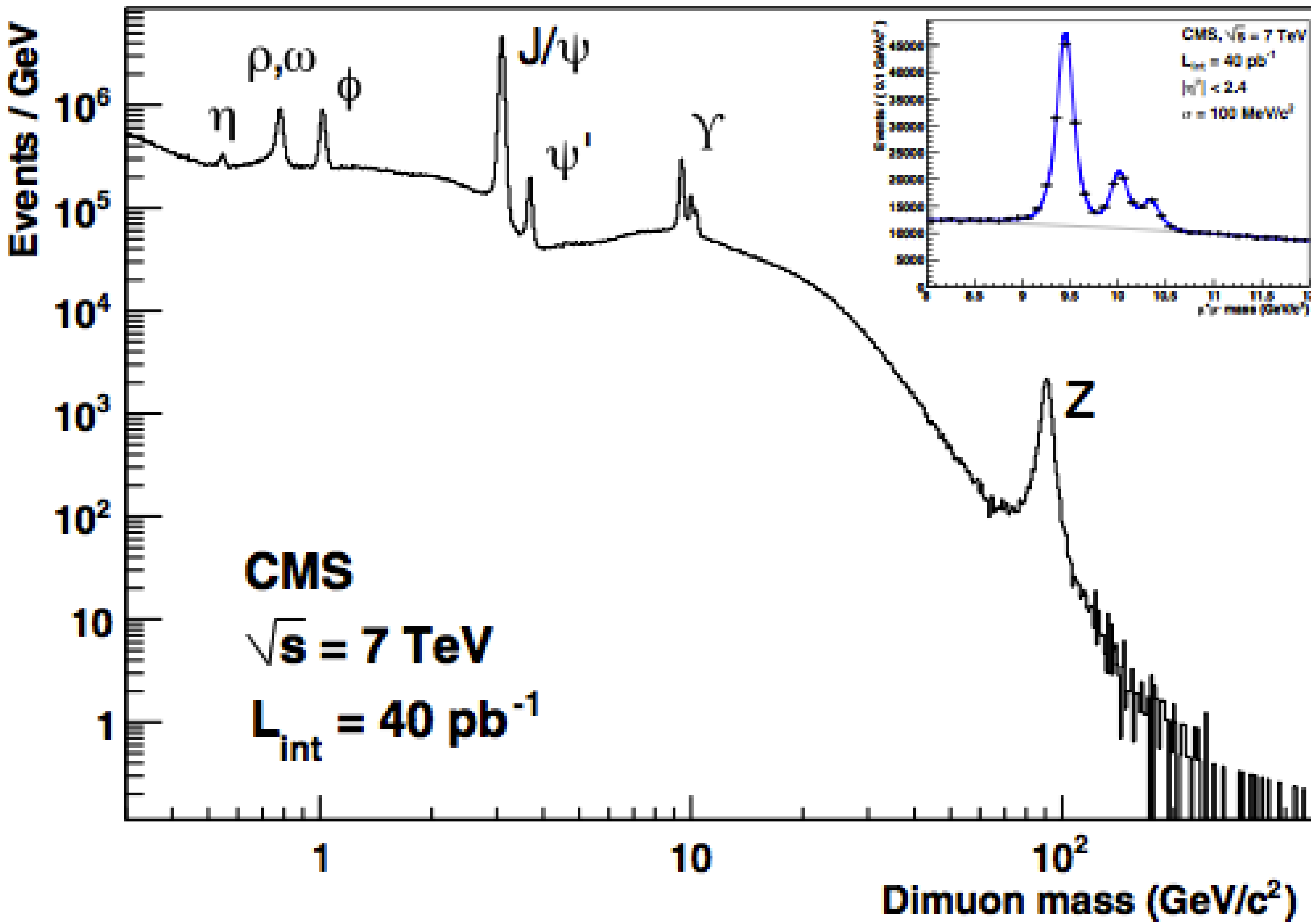

Summary

- **Tracking system is crucial for reconstruction**

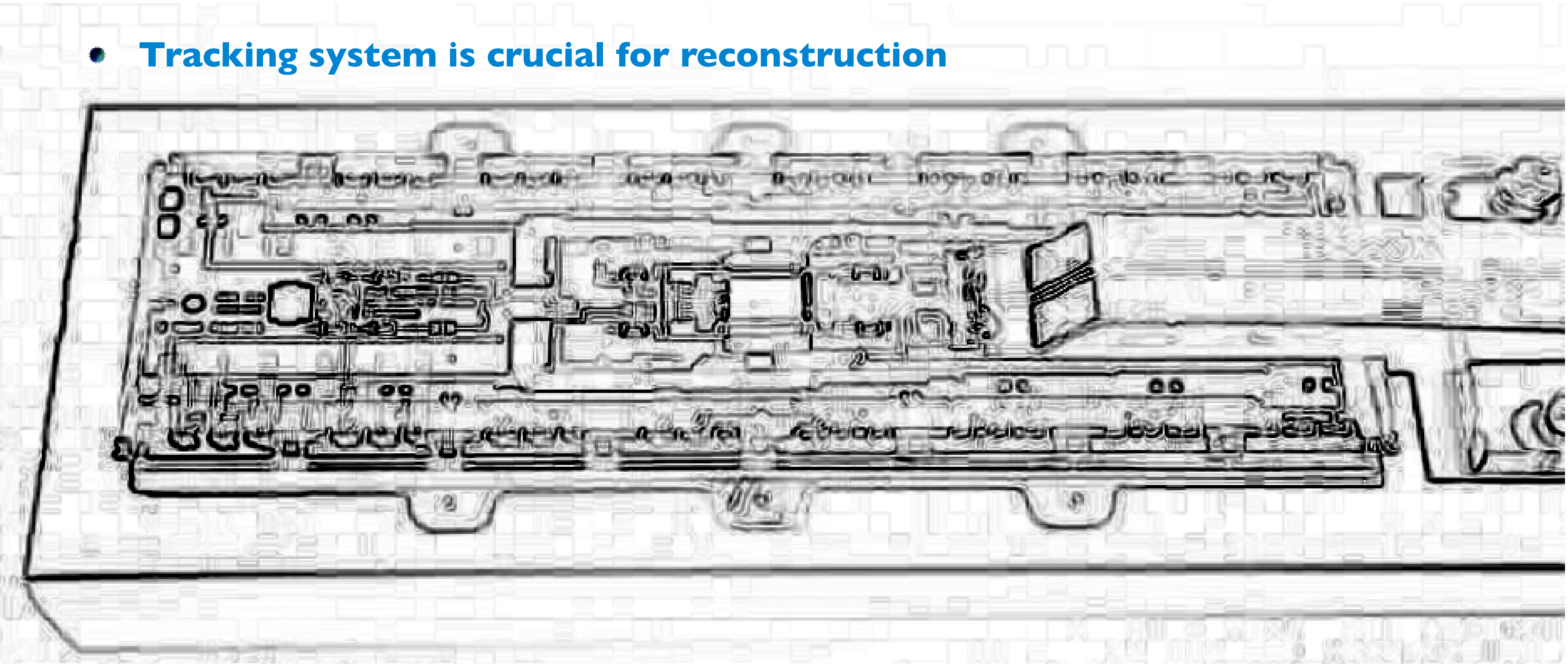

- **Detector design must be physics-driven: optimal reconstruction+performance**

- **Combine powerful tracker with field integral: base for particle-flow**

Bibliography

- Particle data group, "2013 Review of Particle Physics", PRD 86 010001 (2012)
- CMS Collaboration, "The CMS experiment at the CERN LHC", JINST 3 (2008) S08004
- D. Bortoletto, "Detectors for particle physics – semiconductors", Purdue
- A. David, "Tracking and trigger", LIP
- M. Kranmer, "Silicon detectors", HEPHY